

POLITECNICO DI TORINO
Dipartimento di Energia
(DENERG)

Corso di Laurea Magistrale in Ingegneria Energetica e Nucleare

Tesi di Laurea Magistrale

Development and optimization of an
innovative solar atmospheric water
generator



Relatore:

Prof. Marco Simonetti

Correlatore:

Vincenzo Maria Gentile

Candidato:

Marta Trinchieri

Anno Accademico 2018-2019

Abstract

Inadequate water supply is a crucial issue that involves millions of people living in the poorest areas of the World. The technologies associated to water harvesting from the atmosphere are receiving more and more attention due to the possibility of extracting water from the air directly where it is needed, with no extra transportation nor substantial energy supply required.

This work aims to contribute to the realization of an Atmospheric Water Harvesting Prototype based on adsorption material technologies and coupled with a low temperature heat source. The system is integrated with two flat plate solar thermal collectors, installed directly on the prototype. The peculiarity of this system is its versatility, being all contained in a square meter basis, and the possibility of realizing a complete passive system. In order to optimize its performances, a preliminary study on a test-prototype that works with the same thermodynamic principle was conducted. Both the regeneration and the adsorption phases are analysed with the aim of quantifying their performances during a complete daily cycle of adsorption/desorption. Furthermore, energy consumption aspects were studied, in particular specific consumption and efficiency have been calculated.

Thanks to the results obtained, it was possible to realize a model having the newest prototype's characteristics. The model is realized on the software TRNSYS coupled with an external Matlab routine that simulates the adsorption unit. The study was oriented towards the investigation of different possible locations and climates, to concretize where the effective utilization of the prototype could be feasible.

Contents

1	Introduction	8
1.1	The problem of access to water resources	9
1.2	State of the art on water extraction technologies alternative to water harvesting from the atmosphere	11
1.2.1	Groundwater resources	11
1.2.2	Sea-water desalination	13
1.3	Water extraction from the atmosphere	14
1.3.1	Refrigeration-based extraction	15
1.3.2	Sorption material-based extraction	22
2	Test bench prototype: description and preliminary data analysis	26
2.1	Description of the prototype	26
2.2	Data analysis	31
2.2.1	Regeneration	31
2.2.2	Adsorption	35
3	SAWG prototype	43
3.1	Components description	43
4	Model description	51
4.1	TRNSYS model	51
4.2	Matlab routine	57
4.2.1	Silica-gel isotherm adsorption curves	58
4.2.2	Model equations	61

4.2.3	Model algorithm	62
4.2.4	Model validation	67
5	Results	76
5.1	Tunisi sample	76
5.2	Climate zones comparison	79
6	Conclusions	88

List of Figures

1.1	Global water demand in 2000 and 2050	10
1.2	Groundwater formations [6]	12
1.3	Desalination technologies [8].	14
1.4	Prototypes installed in the experimental site in the Ajaccio Gulf (Corsica island,FR) [14]	16
1.5	Schematic of testing facility [15]	17
1.6	[16]	18
1.7	Scheme of the Integrated System [18]	19
1.8	Scheme of the Integrated System [18]	20
1.9	Iso-MHI lines plotted on a psychrometric chart for a condensation temperature of [20]	21
1.10	Fraction of the time out of the 10 years (2005–2014) meteorological data in which the ambient conditions were estimated to be suitable for AMH (e.g. MHI N 0.3), overlaid on the physical and economical global water scarcity map [20]	22
1.11	MOFwater-harvesting system [24]	24
1.12	MOFwater-harvesting system [24]	24
1.13	Prototype scheme and structure of the adsorbent/desorbent matrix [22]	25
2.1	Thermodynamic cycle scheme	27
2.2	Thermodynamic cycle	28
2.3	Prototype scheme with sensors	29
2.4	Prototype scheme	30
2.5	HX-ADS Finned heat exchanger filled with silica gel	30

2.6	Air mass flowrate	31
2.7	RH, temperature and absolute humidity for 20°C group of tests	36
2.8	RH, temperature and absolute humidity for 30°C group of tests	37
2.9	Mass released during the regeneration process for tests at 20°C	38
2.10	Mass released during the regeneration process for tests at 30°C	38
2.11	Specific consumption at different fan regulations	39
2.12	T dew point vs T amb for tests at 20°C	40
2.13	T dew point vs T amb for tests at 30°C	40
2.14	TEST 20	41
2.15	TEST 22	41
2.16	TEST 24	41
2.17	TEST 26	42
2.18	TEST 28	42
3.1	SAWG 3D	44
3.2	Adsorption battery	45
3.3	Condenser + regeneration air circuit	46
3.4	Double four-way valve before being installed	46
3.5	On the left RIG/ADS fans, on the right condenser circuit fans	47
3.6	Functional scheme	49
3.7	Assembled prototype	50
4.1	TRNSYS model scheme	56
4.2	Isotherms of adsorption	59
4.3	Isotherms of adsorption in function of absolute humidity	60
4.4	Temperature dependence of coefficients used for polynomial approximation of adsorption isotherms	61
4.5	Volume fraction variation with respect to p/d ratio [35]	66
4.6	TEST 20-Validation	70
4.7	TEST 22-Validation	70
4.8	TEST 26-Validation	71
4.9	TEST 28-Validation	71

4.10	TEST 32-Validation	72
4.11	TEST 38-Validation	72
4.12	TEST 23 (fan regulation 30%)-Validation	74
4.13	TEST 25 (fan regulation 50%)-Validation	74
4.14	TEST 33 (fan regulation 70%)-Validation	75
4.15	TEST 17 (fan regulation 90%)-Validation	75
5.1	Water content variation	77
5.2	HX-ADS air inlet and outlet	77
5.3	Collector variables	77
5.4	World climate zones	79
5.5	Bangkok	81
5.6	Bluefields	82
5.7	Tunisi	83
5.8	Bamako	84
5.9	Perth	85
5.10	Lisbona	86
5.11	Torino	87

List of Tables

3.1	List of sensors	48
4.1	Pump parameters	52
4.2	Pump inputs	52
4.3	Collectors parameters	53
4.4	Collector inputs	54
4.5	Regression parameter values	58
4.6	Constant k_i values in function of temperature	60
4.7	Constant k_i values in function of temperature	61
5.1	Representative cities for each climate zone	79

Chapter 1

Introduction

Among the *Sustainable Development Goals* emitted by the United Nations, we find "ensure access to water and sanitation for all". Currently millions of people suffer from diseases associated with inadequate water supply, sanitation and hygiene. Water scarcity is generally associated with bad economics or poor infrastructure, this aspect negatively influences food security, livelihood choices and educational opportunities for poor families across the world.

To ensure safe access to drinking water and improve sanitation, there needs to be increased investment and research on freshwater ecosystems and sanitation facilities on a local level in many developing countries. [1] From the document "*Water for a sustainable world*", it is possible to find a specific focus on this issue:

"A watersecure world is more than a goal unto itself. It is a critical and necessary step towards a sustainable future. Progress in each of the three dimensions of sustainable development (social, economic and environmental) is bound by the limits imposed by finite and often vulnerable water resources and the way these resources are managed to provide services and benefits. It is therefore imperative that the role of water is taken into account, when seeking to address all major sustainable development objectives." [2]

Lack of fresh water is mainly diffused in the regions of Northern Africa, Middle East, and Central and Southern Asia. Providing drinking water to arid areas is generally

solved by the following methods [3]:

- transportation of water from other locations;
- desalination of sea water;
- extraction from the atmosphere.

It will be analyzed how extracting water from the atmosphere seems a good solution to provide water to areas in which transportation of water is too expensive and desalination is not possible due to the lack of saline water resources.

Although water is available in abundance on the earth, there is a severe shortage of potable water in many countries. Furthermore, non-renewable energy from oil and natural gas is used to run desalination plants for multi-effect evaporators and a substantial amount of electric power is needed to run reverse osmosis units. Both technologies require large amount of energy and quite complex systems. Nevertheless, these methods are considered as the most diffused for Gulf countries, which suffer from shortage of water but at the same time benefit from the availability of oil as cheap source of energy.

Being nowadays CO_2 emission an issue of environmental concern, it becomes no longer possible to rely on technologies strictly based on fossil fuel energy consumption. Also it is important to emphasise that there are many places where energy is both too expensive and not accessible, sometimes fresh water is required at locations far from the energy grid-lines and so requiring a local source of energy.

A brief overview of the cited technologies will be presented in this chapter.

1.1 The problem of access to water resources

According to the OECD Environmental Outlook 2050 by 2050 water demand will increase by 55%. The main users will be BRIICS (Brazil, Russia, India, Indonesia, China, South Africa) and developing countries which respectively contribute with a 700% and 400% increase. As shown in Figure 1.1, the main needs come from the increase in the domestic, manufacturing and power sector, combined with the increase

of population, expected to be up to 33% concentrated in developing countries [2].

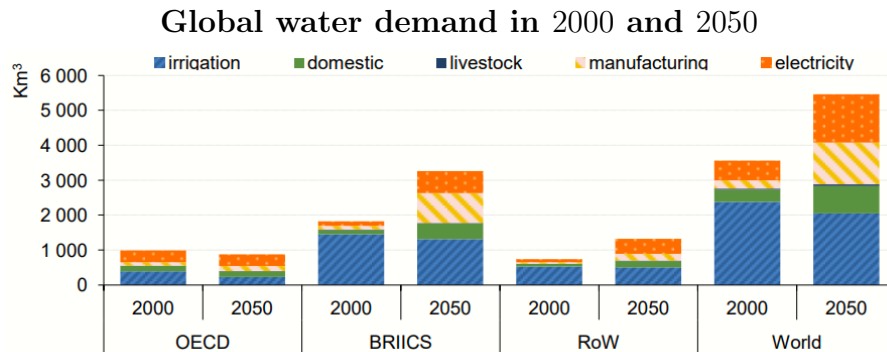


Figure 1.1: Global water demand in 2000 and 2050 ¹

Cities are the areas in which this phenomenon is the most relevant: according to UNDESA report [4], in 2014 54% of the global population lived in cities and by 2050 it will raise up to 65%. Cities impact on the hydrological cycle in two ways:

- extending impenetrable surfaces which does not allow the natural recharge of groundwater and aggravates flood risks;
- discharging polluting water bodies inside untreated wastewater.

Unfortunately, since much of the water consumed by cities generally comes from outside city limits and the pollution generated tends to flow outside too, the impact of cities on water goes beyond their boundaries. Rapid urbanization, increased industrialization, and improving living standards generally combine to increase the overall demand for water in cities.

On the other hand, cities, as poles of innovation, provide opportunities for more sustainable use of water, for example treating used water and enabling it to be used again. Furthermore, the concentration of people in small areas can reduce the cost of providing services such as water supply and sanitation. Cities can also connect with their hinterlands and support the protection of water resources in their surrounding areas by actively engaging in watershed management or providing PES (Payments for Ecosystem Services).

Between 1990 and 2012, the number of people in urban areas without access to a

drinking water source increased from 111 million to 149 million [5]. Access to drinking water is more critical where the most rapid urbanization is taking place, sub-Saharan Africa is one of the most critical areas: in this region, the percentage of people who had the access actually decreased from 42% to 34% [5]. This clearly indicates that access to drinking water sources continues to be a major problem in cities in developing world.

Similar to trends in drinking water, the number of people living in cities without access to sanitation increased by 40%, from 541 to 754 million, between 1990 and 2012 [5]. Therefore, although sanitation coverage is generally higher in urban areas, because of rapid urbanization, increasing numbers of urban residents, particularly the poor, are unable to access improved sanitation. Also, due to higher population densities in urban areas, the health consequences of poor sanitation can be pervasive. In urban Cambodia, for example, 54% of the people in the poorest quintile still defecate in the open, while among the richest 40% of the population, this has gone down to zero.

1.2 State of the art on water extraction technologies alternative to water harvesting from the atmosphere

Up to now, the solutions available to satisfy the increasing water demand are: to dig deeper to access available water resources, mainly groundwater resources, or exploit innovative solutions such as sea-water desalination [2].

1.2.1 Groundwater resources

Groundwater is the water found underground in the cracks and spaces in soil, sand and rock; it is stored in and moves slowly through geologic formations. Groundwater supplies are recharge, by rain and snow melt that flows down into the cracks and crevices underneath the land's surface. Water in aquifers, is brought to the surface naturally through a spring or can be discharged into lakes and streams [6]. Groundwater can also be extracted through a well drilled into the aquifer, as shown in figure 1.2.

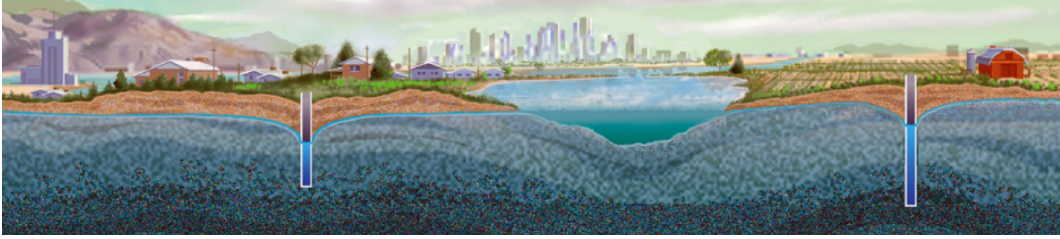


Figure 1.2: Groundwater formations [6]

In last decades groundwater has become one of the most important natural resources for many countries. It happens that groundwater is available in places where there is no surface water. The main advantages related to the use of groundwater are:

- better quality, being protected from possible pollution and possible infection;
- lower intermittency, since it is less subject to seasonal and perennial fluctuations;
- greater availability, being spread over large regions more uniformly than surface water.

Groundwater is the only source of water supply for some countries in the world (Denmark, Malta, Saudi Arabia, etc.) [7]. It represents the substantial part of water resources in the other countries. As an example, in Tunisia, groundwater is 95% of the country total water resource, in Belgium it is 83%, in the Netherlands, Germany and Morocco it is 75%, and in most of the European countries it is over 70% of the total water consumption.

In countries with arid and semiarid climate groundwater is widely used for irrigation. About one-third of the landmass is irrigated by groundwater. Out of the total irrigated land in the United States of America, 45% is irrigated by groundwater, 58% in Iran, 67% in Algeria, and in Libya irrigated farming is wholly based on quality groundwater. High quality groundwater is mainly used in domestic applications and drinking water supply. It results possible to use fresh groundwater for other purposes, such as industry and irrigation, only having an acceptable availability of groundwater reserves. It has to be sufficient for meeting the available and perspective demand in drinking water and by special permission of nature-protecting institutions.

However, intensive groundwater exploitation, its considerable withdrawal under mineral deposits mining and different drainage measures, human activities impact on its quality and resources put in the agenda the problem of groundwater rational use, the main task being to work out scientific bases and technique of its resources management.

1.2.2 Sea-water desalination

Desalination is a process that involves the separation of saline water in two parts using different forms of energy: one part is characterized by a low concentration of dissolved salts (fresh water), the other has a much higher concentration of salts comparing it to the original water (brine concentrate) [8].

The majority of water desalination processes are divided into two types: phase change thermal processes and membrane processes. Thermal processes are based on the principles of evaporation and condensation, water is brought to evaporation where the salt is left behind and vapour is taken away and condensed in another heat exchanger to produce fresh water. Membrane technologies use a relatively permeable membrane to move either water or salt to induce two zones of different concentrations in order to produce fresh water. The membrane is a thin film of porous material that allows water molecules to pass through it and at the same time prevents the passage of larger molecules (salt, bacteria, metals etc.)

There are also some alternative technologies that includes freezing and ion exchange, but they are less used. All the processes can be both driven by conventional or renewable energy sources.

In figure 1.3 we have an overview of the processes mentioned.

The main drawbacks related to this kind of technologies are related to the energy needed to make them work. Large commercial desalination plants that use fossil fuels are diffused in most of the countries suffering from water shortages. For instance, a number of oil-rich countries use fossil fuel to supplement the energy for water desalination supply. In contrast people in many other areas of the world have neither the financial nor oil resources to allow them to develop in a similar manner.

The typical solutions become economically feasible for large plants only. Moreover,

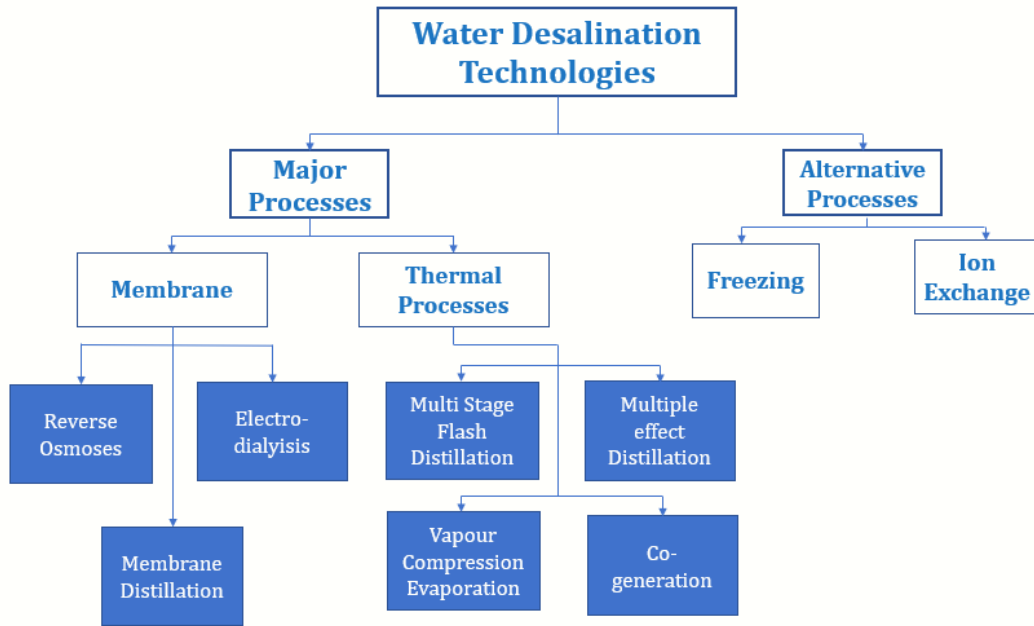


Figure 1.3: Desalination technologies [8].

they are quite energy intensive, being based on the use of fossil fuels and, causing a large carbon footprint of the produced fresh water. Further on, it appears evident that persons that lack the access to water will also likely lack the access to electricity or other fuels to power decentralized solutions. [9].

1.3 Water extraction from the atmosphere

The atmosphere , containing $12,900 \text{ km}^3$ of fresh water in form of water vapor can be considered as a huge and renewable source of fresh water.

Many studies in literature [10], [11] [12] show that it is a promising solution to bring this technology in those regions who lack of access to proper infrastructure and economic resources of extraction of water. As already seen, desalination plants seem to be unappropriate being energy intensive, based on the use of fossil fuels and causing a large carbon footprint of the produced fresh water. Moreover, many of the regions in need of water are located in the developing countries where solar radiation has a high incidence, so it results useful to couple the techology of water extraction with the solar

resource.

In literature, we find different way to process air to extract water molecules from the atmosphere. They are generally based on the phase change from vapor to liquid. The studies normally investigate different humidification and dehumidification techniques in which air is used as a medium to carry water in form of vapor.

Among these we find two main valid options [13]:

- the use of a refrigeration cycle based on vapor compression heat pumps or absorption chillers, to cool the air under dew point to cause condensation of the vapor content of the air;
- use sorption materials to subtract water vapor contained in the atmosphere. Afterwards the material is regenerated and the water is condensed at ambiend temperature.

1.3.1 Refrigeration-based extraction

Concerning the refrigeration-based extraction one of the first technology proposed was by radiative cooling [14]. It consist of extracting the atmospheric moisture by cooling making an air stream go under its dew point following contact with a cold surface. In terms of energy, this process involves a latent heat release close to $2500kJ/kg$ as well as sensible heat interaction between the air and the surface. It becomes necessary to keep the temperature of the surface below the dew point to ensure the condensation process, and so a heat flux is necessary to compensate the heat exchange of the surface. Radiative cooling towards the night sky drives natural amospheric moisture extraction via the formation of dew on surfaces.

An example of the prototypes used in the experiments is given in figure 1.4:

In general, the process limitations are given by the rate of radiative heat exchange, the weather and the surface properties. In particular on weather conditions it depends the ratio of latent and sensible heat exchange between the surface and the air. When the dew point temperature is much lower than the air temperature most of the radiative cooling is consumed by a sensible heat exchange. On the other hand, if the difference between ambient air and dew point temperature it is more difficoult to get

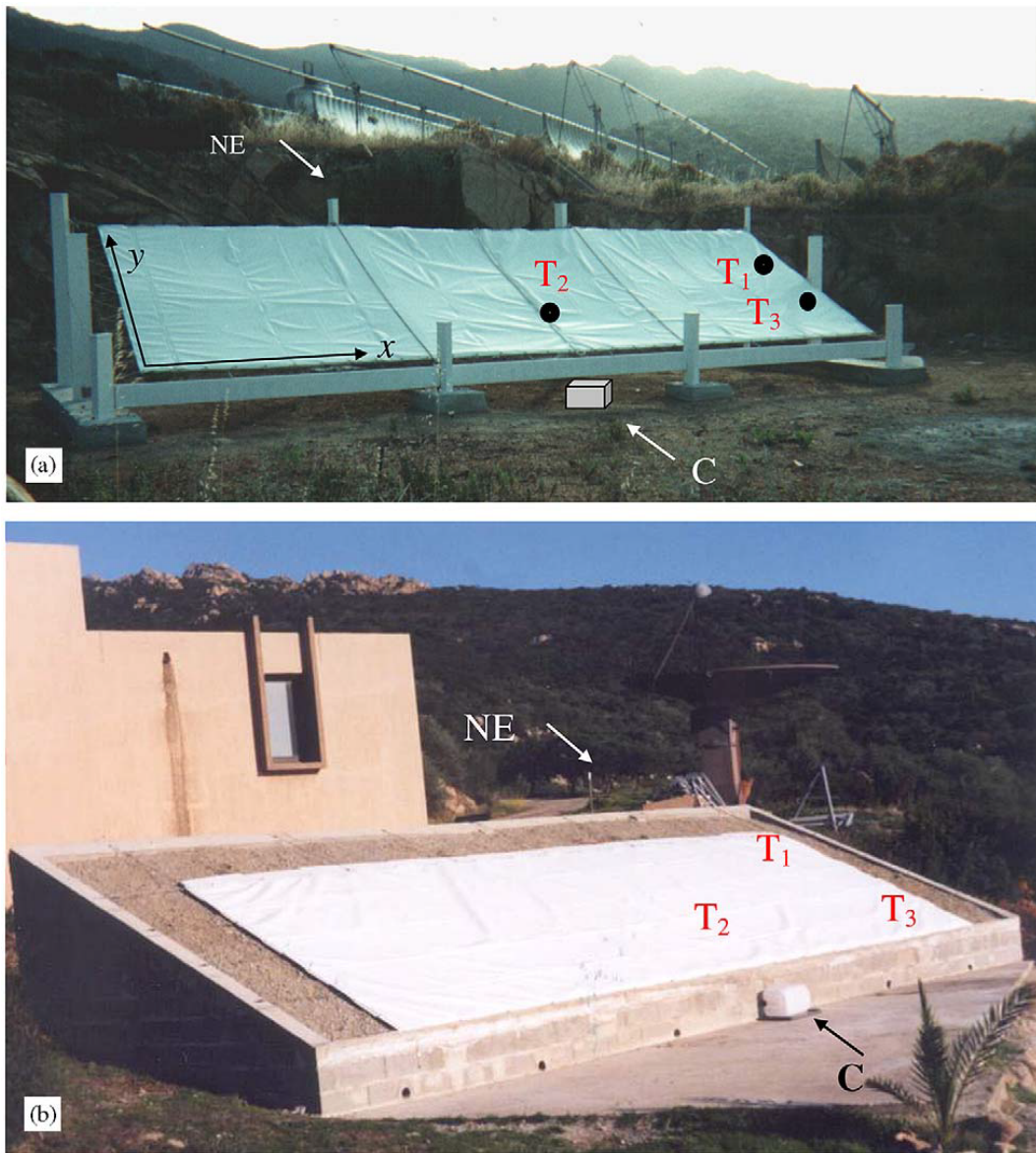


Figure 1.4: Prototypes installed in the experimental site in the Ajaccio Gulf (Corsica island,FR) [14]

any significant dew yield. Anyway, passive dew harvesting can be only a supplementary water source in regions with favorable conditions.

Another possible solution to harvest atmospheric humidity is by active cooling of ambient air, using a cycle driven by electricity. Although supplying energy is a solution to avoid the limitation of passive radiative cooling, the efficiency of the process is still highly dependent on the meteorological conditions.

This type of systems are currently available in the market. Their main application is for emergency and when relatively small amounts of fresh water are required.

In literature, some of the available systems in the market have been analyzed [15] to show their performances and limitations. An experimental procedure was developed following ASHRAE and ANSI/AHRI standards. The aim was to characterize the behaviour of the systems by measuring their water harvesting rate (energy supply needed to produce 1L of fresh water) and input electrical power needed by different residential units. Three commercial units have been studied and compared, they were taken from USA, Canada and China markets. These systems were chosen in such a way they had the same technical characteristics: they are able to produce 30l/day and have a nominal power of 1500W.

The experiments were done in an environmental chamber in the research laboratory at Simon Fraser University to investigate different climatic conditions. The environmental chamber is able to reproduce wide ranges of temperatures and relative humidities. A schematic overview of the experimental set-up is shown in figure:

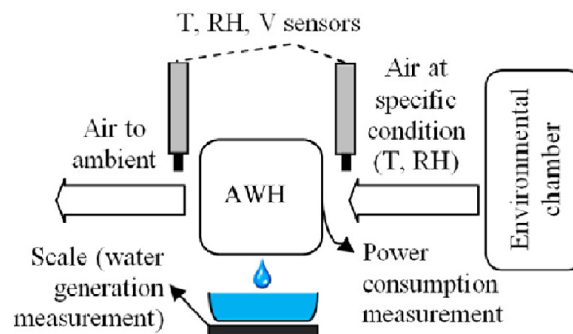


Figure 1.5: Schematic of testing facility [15]

Results show that the Water Harvesting Rate is contained within a range of 1.02 kWh/l in hot and arid climates and 6.23 kWh/l in cold and humid climates.

Some ways to improve the direct cooling technology have been investigated as well. One option is to couple the cooling system with a selective membrane that separates the water vapor from the other gases [16] [17]. In this way a specific cooling of the concentrated vapor is enhanced and it makes the process more energy efficient avoiding the cooling of the whole air stream. To investigate these type of systems a prototype

was realized. It is shown in figure:

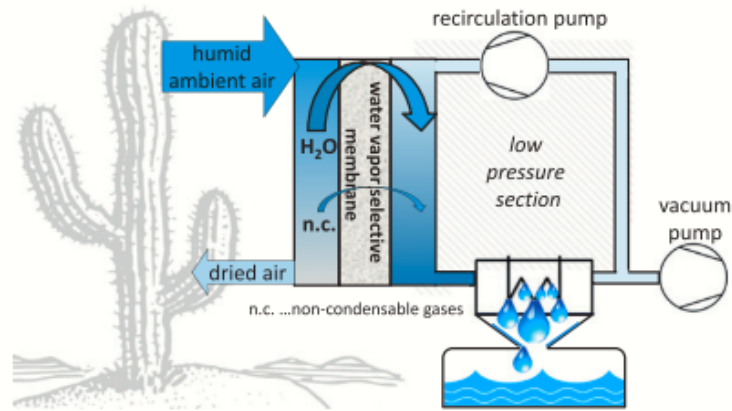


Figure 1.6: [16]

The driving force of the process is a partial pressure difference, it is maintained thanks to a condenser and a vacuum pump. The pump removes all the non-condensable gases that leak into the system. It was also shown how, introducing a low-pressure, recirculated sweep stream, the total permeate side pressure can be increased without compromising the water vapor permeation. The advantages and disadvantages of using vacuum and sweep stream are investigated and a combination of these two is introduced, in order to obtain an optimal condition for water harvesting. In this way, even in presence of leakages, it is possible to lower the power requirement of the vacuum pump.

The technical specifications of the prototype are: a nominal power of 62 kW, a daily production of water of $9.19m^3/day$ that means $583MJ/m^3$.

Another option that has been investigated is to couple the direct cooling water harvesting with a conventional HVAC system. In this way, it is possible to contemporarily use the cooled air for refrigeration [18] [19]. In this research, the humid air cooling process below the dew point to cause the condensation is combined with the air conditioning. A case study is taken into account and compared with a traditional HVAC system to show the advantages achievable with the improved one. The case study takes into account the HVAC system of an existing hotel placed in sub-tropical, arid

climate. In this case, the production of water is meant to be used for the building needs.

A scheme of the integrated plant is shown in figure.

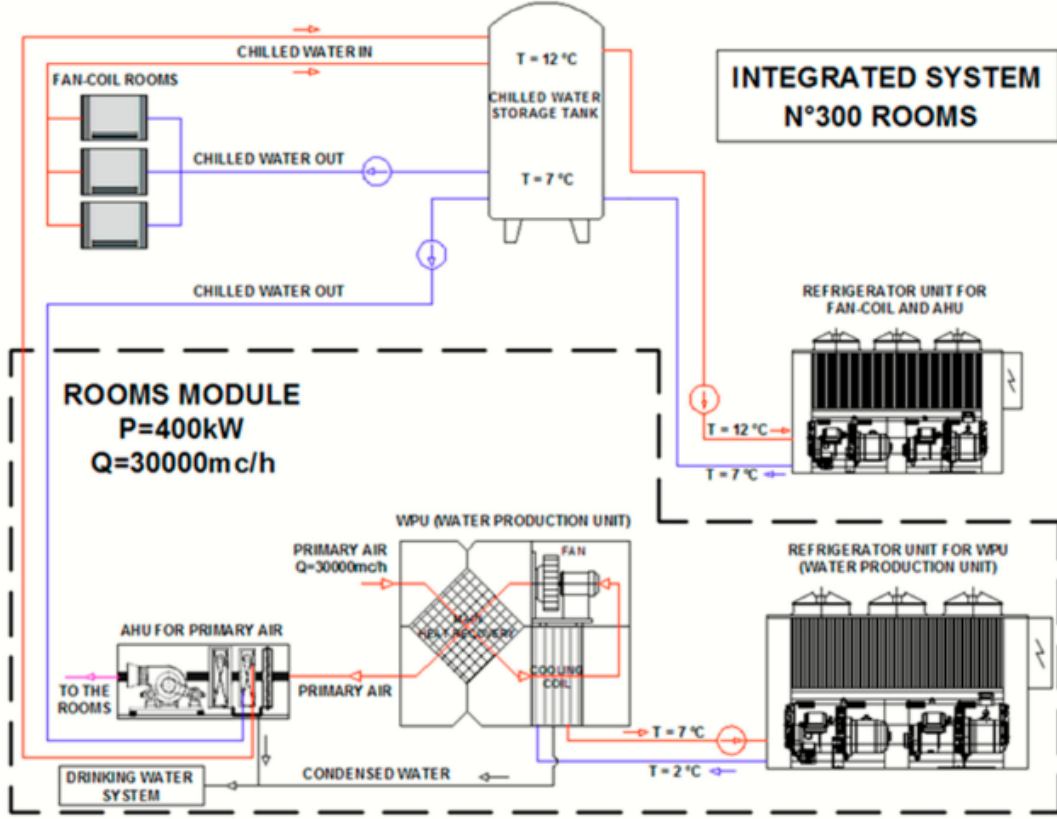


Figure 1.7: Scheme of the Integrated System [18]

Calculation on daily water production and energy consumption of the traditional solution (TS) and the integrated solution (IS) have been studied. In table below is possible to get an idea of the scale and the performances of the system:

An index has been introduced to try to estimate the energy performances of this technology [20]. The index is called MHI (Moisture Harvesting Index). It is calculated as:

$$MHI = \frac{h_{fg}}{q^*_{tot}}$$

where:

- h_{fg} is the enthalpy of condensation [kJ/kg_w]. It generally varies only slightly for the range of condensation temperatures found in commercial application, so in the article it is assumed a constant value equal to $2492 kJ/kg_w$;

	TS - Typical System		IS - Innovative System	
	Rooms	Common areas	Rooms	Common areas
External air [m ³ /h]	30000	150000	30000	150000
Recirculated air [m ³ /h]	0	150000	0	150000
Recovered heating power [kW]	0	361.5	215	1340
Cooling power battery packs [kW]	565.7	3463	517	3650
Post-heating battery pack [kW]	82.2	123.5	0	337.5
Electric power for refrigeration [kW]	177.9	1117.1	180.9	1248
Fans electric power [kW]	16.2	205.6	23.9	231.5
Chilled water pumps electric power [kW]	7.5	55	7.7	55
Post-heating water pump electric power [kW]	1.2	1.0	0	5,5
Condensed water [m ³ /day]	11.0	66.4	12.4	72.2
Energy consumption [kWh/day]	4867	33089	5100	36960
TOTAL ENERGY CONSUMPTION	37956 kWh/day		42060 kWh/day	
TOTAL CONDENSED WATER	77.4 m ³ /day		84.6 m ³ /day	

Figure 1.8: Scheme of the Integrated System [18]

- q^*_{tot} quantifies the total heat required to be removed from the air for the production of 1 kg of liquid water and is calculated as:

$$q^*_{tot} = \frac{h_o - h_i}{r_i - r_i} [kJ/kg_w]$$

being $h_o - h_i [kJ/kg_a]$ the specific enthalpy difference considering an isobaric process referred to 1kg of air. Since we are interested in calculating the heat required for the transformation of water, the difference of enthalpies is divided by $r [kg_w/kg_a]$ that is the air moisture content. In this way we obtain a quantity relative to 1kg of water.

The MHI mainly depends on three parameters: the thermodynamic conditions of the air at the inlet (T_i and r_i , where T_i is the ambient air dry bulb temperature at the inlet) and the condensation temperature T_o . Being the condensation temperature a fixed parameter set during the design phase, the *MHI* only depends on the thermodynamic conditions of the air at the inlet.

In this way, it is possible to draw up different behaviours of *MHI*: high *MHI* characterizes warm and very humid ambient conditions, where the requirement for sensible heat removal is small and the overall efficiency of the process is relatively high. On the other hand, low *MHI* is typical of ambient conditions that bring to high demands for sensible heat removal and low moisture condensation yield.

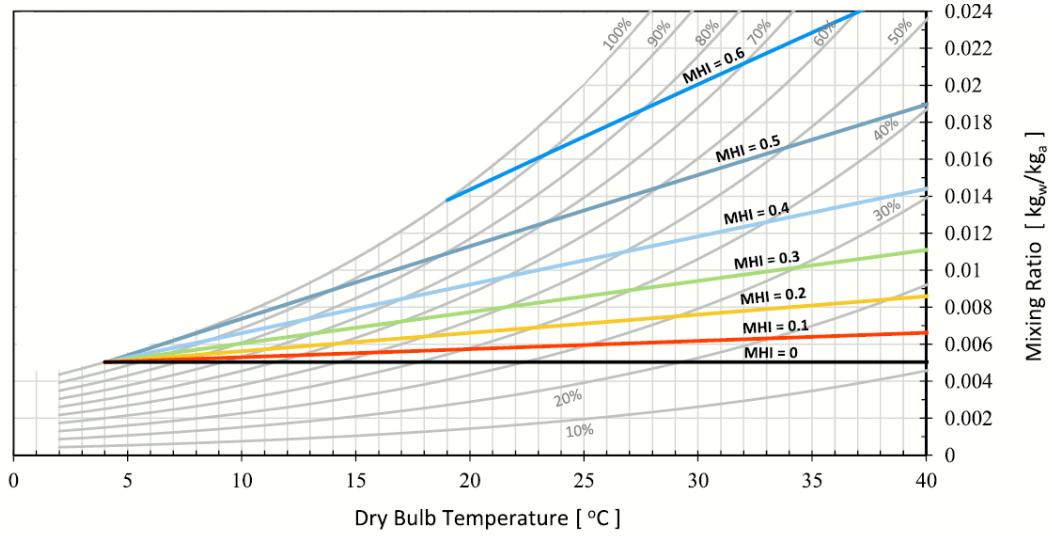


Figure 1.9: Iso-MHI lines plotted on a psychrometric chart for a condensation temperature of [20]

From 1.9, it is possible to have an overview.

Being *MHI* daily and seasonally variable, it is found that continuous operation of a device based on Atmospheric Moisture Harvesting by direct cooling is energetically and economically possible only in specific regions. In particular, the favorable regions are found to be the tropical ones since they experience high relative humidity and stable temperatures throughout the year. For other regions, in order to decrease the energy requirements it would be preferable to avoid operation of the system when *MHI* is low, and so shifting from continuous to non-continuous operation. Clearly, there will be some drawbacks of such intermittent operation mode: smaller water production and mechanical problems due to discontinuous operation cycle.

It was possible to observe that refrigeration-based technologies have a limitation due to climatic conditions. In arid regions, due to the low humidity, the dew point temperature is lower than 15°C and even below 0°C in extremely dry desert climate. This condition makes it infeasible in terms of practical implementation with a huge energy consumption [21]. To supply this high request it would be needed to install a lot of PV plate, in terms of making the system to be passive, which implies high cost and maintenance. Furthermore, conventional refrigeration still uses chlorofluorocarbons (CFCs), which contribute to global high altitude ozone depletion [22].

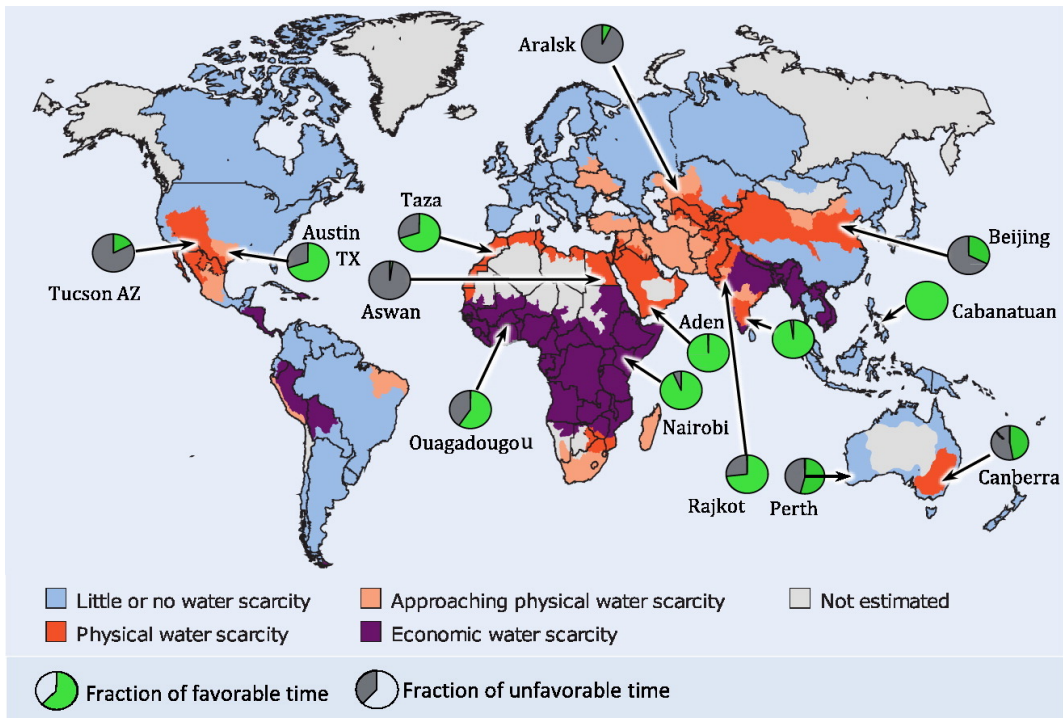


Figure 1.10: Fraction of the time out of the 10 years (2005–2014) meteorological data in which the ambient conditions were estimated to be suitable for AMH (e.g. MHI N 0.3), overlaid on the physical and economical global water scarcity map [20]

1.3.2 Sorption material-based extraction

Sorption-based water harvesting systems adopt selective water sorbent to separate water vapor from atmosphere [23]. Solar driven solid sorption water vapor uptake is one reasonable way for water harvesting in arid area since it can work under 0°C air dewpoint conditions.

Ideally, a water harvesting unit should operate with a sorption material that is able to take up and release water with minimum energy requirements and that is powered by low grade energy sources, like sunlight as to result favorable for applications in sunny regions.

In general, in systems based on this technology, the water vapor in air is adsorbed into the adsorption bed at night when the temperature is low and the relative humidity is high. On the other hand, the bed is regenerated by means of solar energy during the daytime, desorbing the adsorbed water. By recirculating the air a high vapor content is generally obtained and is then condensed into a water cooling condenser.

The selection of solid sorbents is a very crucial step for fresh water production based on sorption. Different materials have been investigated in literature to be used as sorption material. In literature, it is possible to find different studies using: MOF and ACF + salt combination.

MOFs MOFs (metal-organic framework), have been studied as possible sorbent material to couple with this technology. In particular the attention was focused on MOF-801 ($Zr_6O_4(OH)_4(fumarate)_6$) [24]. They reported a device, that uses MOF, able to harvest 2.8L of water per kg of MOF per day at 20% of RH. It is supplied by nonconcentrated solar radiation, as to say less than $1000W/m^2$ requiring no additional power input. The use of MOFs becomes interesting from the energy consumption point of view since an isotherm with a strong increase in water uptake within a restricted range of RH is obtained. In this way, we get maximum regeneration with minimal temperature increase. According to the study, MOF-801 shows suitability for regions such as North Africa, where RH is 20% and also India with $RH = 40\%$, where regeneration temperatures of $65C$ were possible. Once water vapor is absorbed into the MOF, solar energy is used to release the adsorbate. Water is then collected using a condenser that uses ambient temperature. For this type of application this sorbent material shows several chemical advantages:

- well-studied water-adsorption behaviour at molecular scale;
- good performances due to aggregation of the water molecules into clusters within the pores of the MOF;
- stability and possibility of recycling;
- available and low cost.

A scheme of the prototype is given in figure 1.11.

The scheme is composed of a MOF layer and a condenser, undergoing solar-assisted water-harvesting and adsorption processes. During water harvesting (left), the desorbed vapor is condensed at the ambient temperature and delivered through a passive heat sink, requiring no additional energy input. During water capture, the vapor is adsorbed on the MOF layer, transferring the heat to the ambient surroundings (right).

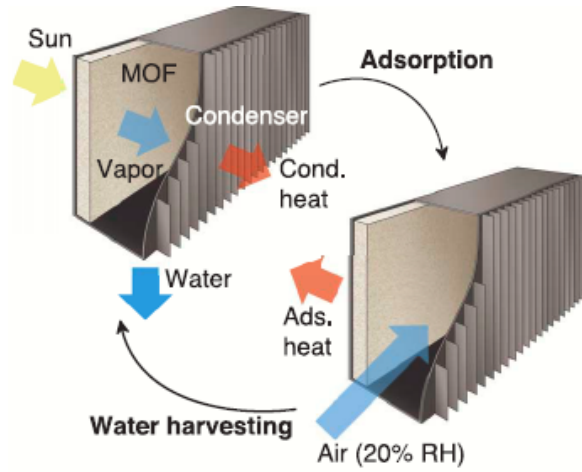


Figure 1.11: MOFwater-harvesting system [24]

The range of application of sorption/desorption phases is from 10°C or lower to 30°C



Figure 1.12: MOFwater-harvesting system [24]

or higher which incredibly reduces the energy consumption for the production of a large amount of water. [22]

ACF + Salt The active Carbon Felt matrix coupled with LiCl, seems to be a promising solution. ACF generally shows the advantage of a huge surface area ($1380m^2/g$) and fast intraparticle adsorption kinetics. The surface is particularly homogeneous being the micropores uniformly distributed on the fiber surface, with average pore size from 0.1 to 2.0 nm. This microstructure is the direct responsible for the strong capillarity of the material [25]. A possible combination with ACF matrix is the combination with a salt. For example with $CaCl_2$ the water uptake is around 1.7 g/g, which is a good result, but this sorbent has the drawback of becoming soft after sorption so its unstable structure makes it impossible to use it. Another commonly used salt is LiCl [26] [27]. It was observed that in this configuration the materials shows good water uptake performances and large desorption quantities (0.65 g/g) at $77^\circ C$ and 20% RH.

A prototype was built and tested with this material combination. [22] With 70kg od adsorbent in a $1.0 \times 0.75 \times 0.3$ m, it was possible to collect 38.5 kg of fresh water per day with a specific consumption of $7.2 MJ/kg_w$. In prototype also the structure of the bed was optimized, using a scalable modular matrix with sinusoidal honey comb structure.

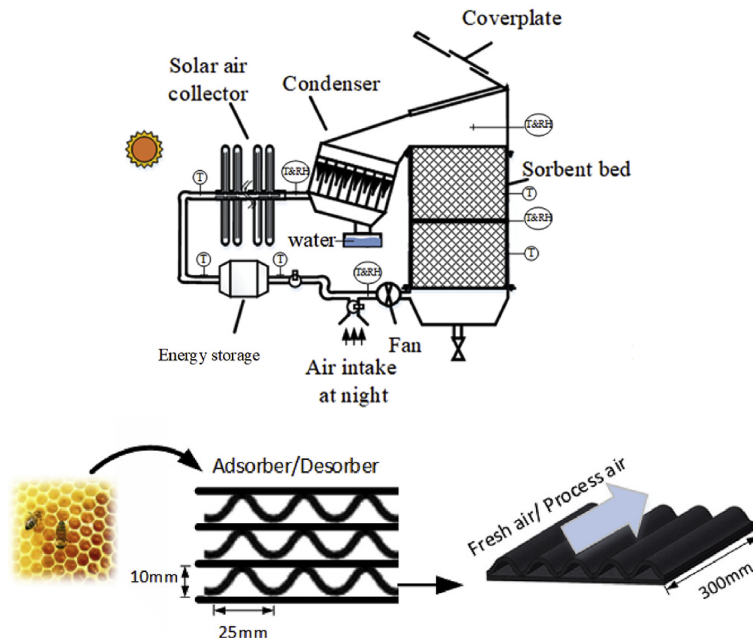


Figure 1.13: Prototype scheme and structure of the adsorbent/desorbent matrix [22]

Chapter 2

Test bench prototype: description and preliminary data analysis

In the laboratory of Energy department at Politecnico di Torino, two prototypes based on sorption materials have been assembled. One, the so-called test-prototype was assembled in order to test its performances; the second one was built in a more compact way in order to prove its feasibility for real applications. This second type will be analyzed in detail in the following chapters.

2.1 Description of the prototype

The test prototype assembled in the laboratory of Energy department of Politecnico di Torino has the purpose of extracting water from atmospheric air.

The System can work alternating two different phases that are:

- Adsorption: humidity in ambient air is absorbed by the adsorption material, that for this prototype is Silica gel;
- Desorption: adsorbent material is heated up using a low temperature energy source. In this way, it releases the moisture collected during the adsorption process.

The hot and humid flux leaving the heat exchanger is then condensed in a dry cooler at the outdoor ambient temperature. It was connected to a UTA to keep the temper-

ature of the whole process constant and experiment different testing temperatures.

A schmatic of the process is given in figure below:

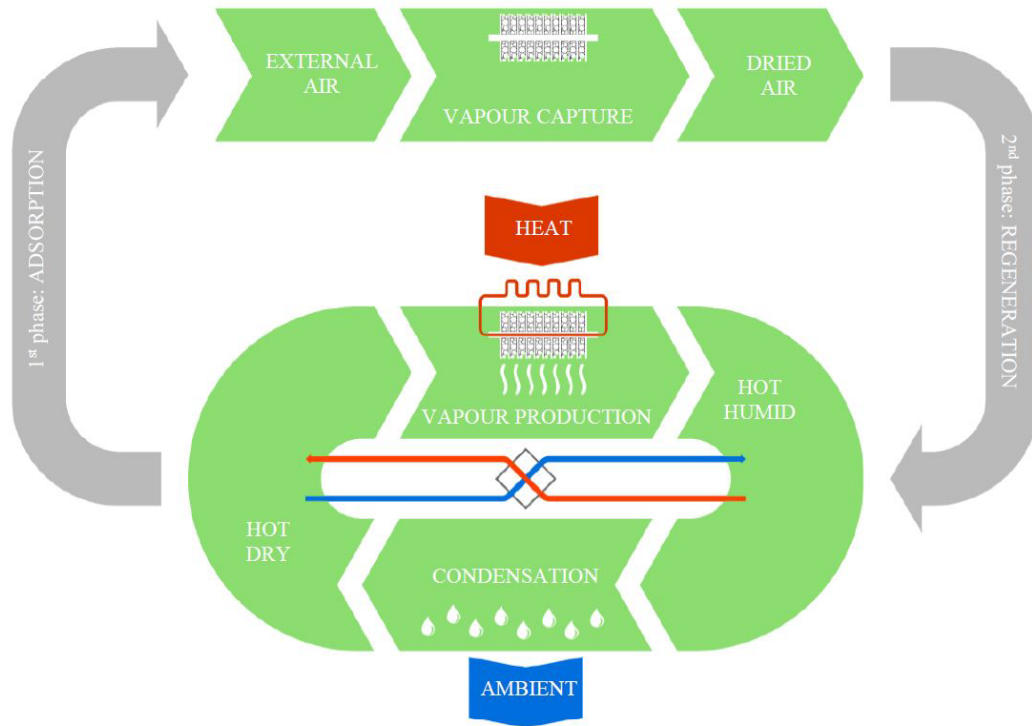


Figure 2.1: Thermodynamic cycle scheme

It was observed that to have significant production of water during condensation it is necessary to reach a certain level of humidity and temperature for the air stream going through the condenser in such a way that the dew point temperature of the stream is always higher than the ambient air. Generally humid air going through adsorption/desorption processes moves along isenthalpic transformations. This implies that the variation of moisture content inside the air stream is always linked to a temperature difference. In particular, during adsorption moisture content reduces and air temperature increases and viceversa for regeneration processes. Being the goal of this system the water production, it can be observed that through this kind of thermodynamic transformations the amount of moisture collected is quite poor considering to have a condensing stream at ambient temperature, for instance at 35°C , like a possible application temperature could be. In this case, the saturation point corresponds to about $36.5 \text{ g}_v/\text{kg}_a$ (point 3 in figure 2.2). Moving on an isenthalpic transformation,

in order to reach the points on the saturation line an inlet desorption air at 50°C and same moisture content of point 3 is needed (point 1). However, a very reduced amount of moisture will be condensed.

The solution is to perform an isothermal transformation, in such a way that the

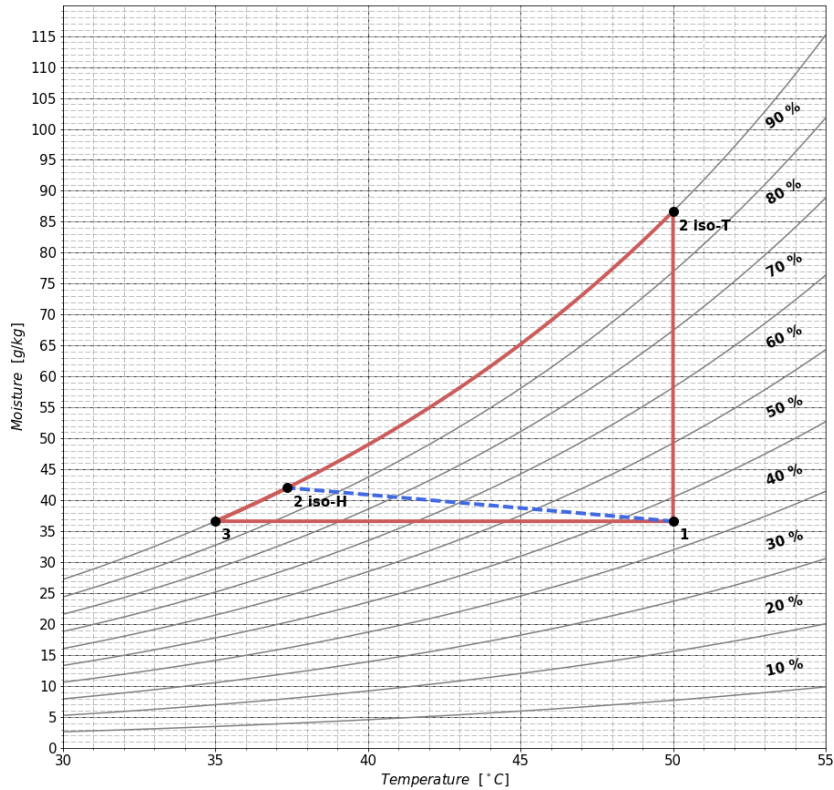


Figure 2.2: Thermodynamic cycle

humidity content difference on saturation line between point 2 and 3 is much higher. In the example shown in figure, it would change from g_v/kg_a of the isenthalpic transformation to more than 40 g_v/kg_a of the isothermal one. To realize such transformation a system exchanging heat and mass is needed, this is possible in a finned heat exchanger filled with adsorption material. The heat for the adsorption is supplied by water circulation at temperatures of 50-80°C. A fan circulates the air flow through the HX-ADS in a closed loop, to permit the continuous subtraction of water from sorption

material.

After this stage, the air is cooled down in a condenser that is subdivided into two parts. The first one consists of a heat recovery the reheat the regeneration stream exiting the component, the second part is the actual condenser that works with external ambient air.

Going through the technical aspects of the prototype, it is possible to state that it is able to collect around 2 liters from the treatment of an air volume of 100 m^3 . The adsorption system contains about 20.5 kg of silica gel grain with average diameter of 3 mm. The heat is supplied by a circulation of water between $50\text{-}80^\circ\text{C}$ produced by an electric resistance of 1.25kW.

The air flow is moved by a centrifugal fan at variable velocity regulation with a maximum power consumption of 43W and air flow rate range $0\text{-}100 \text{ m}^3/h$. All the components are connected by a flexible duct.

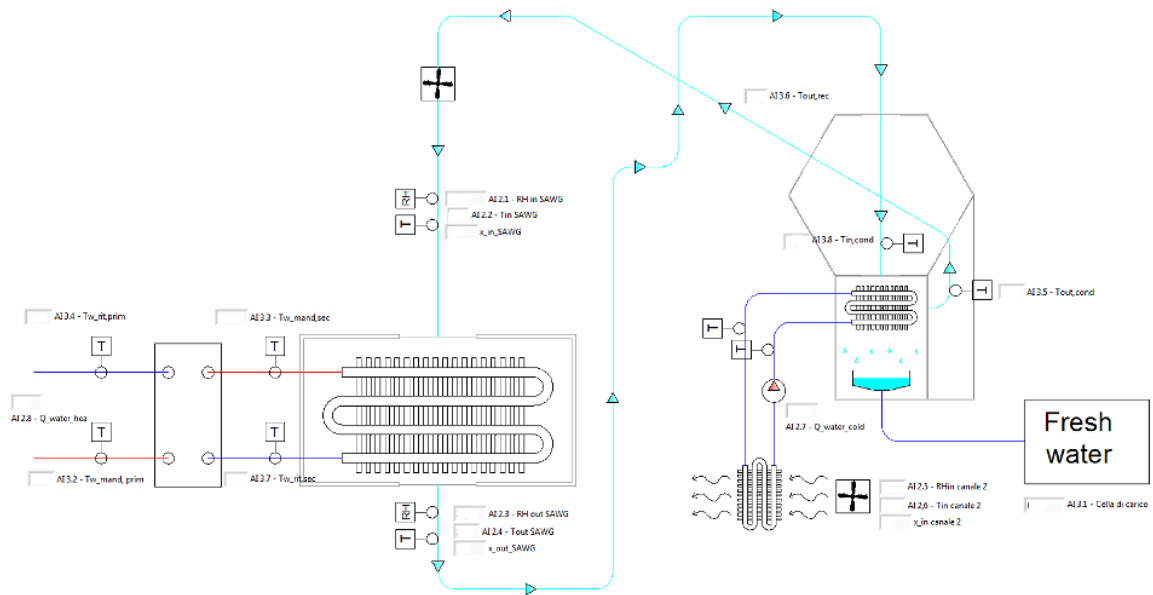


Figure 2.3: Prototype scheme with sensors

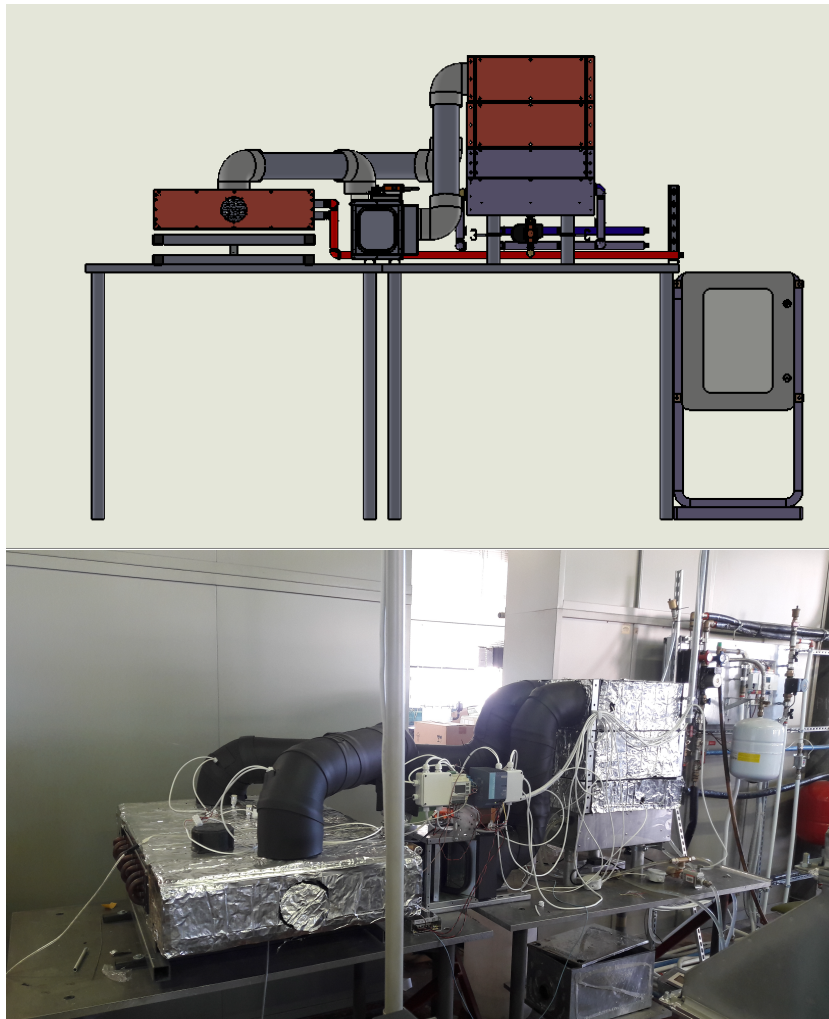


Figure 2.4: Prototype scheme



Figure 2.5: HX-ADS Finned heat exchanger filled with silica gel

2.2 Data analysis

A data analysis was performed in order to study the operation of this system. In particular, the regeneration and adsorption processes are treated separately.

For both processes, in order to derive the air flow rate a regression was obtained performing tests at different fan regulations and measuring the corresponding speeds.

The second degree polynomial obtained are:

$$RIG : y = -0,0042x^2 + 1,0017x - 7,9956 \quad (2.1)$$

$$ADS : y = -0,0029x^2 + 0,9621x - 5,8062 \quad (2.2)$$

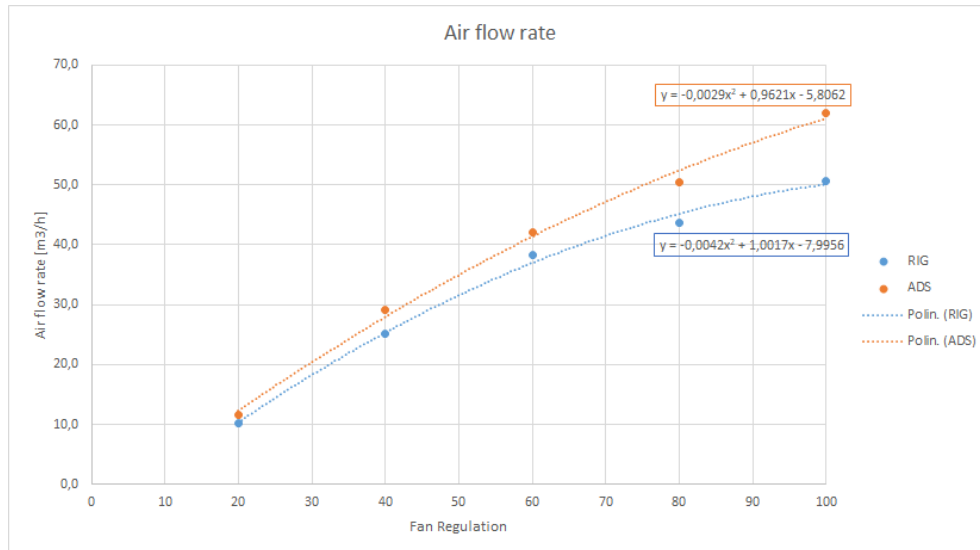


Figure 2.6: Air mass flowrate

2.2.1 Regeneration

Regeneration test analysis was performed dividing the tests into two main groups according to the ambient temperature set by the UTA unit. The two groups are performed at 20°C and 30°C ambient temperature. For each group of tests different fan regulations were taken into account, the fan was regulated at 30%, 50%, 70% and 90%. A first comparison was made plotting the relative humidity, the temperature, calculating the absolute humidity and the mass balance for the water released during the

regeneration. Results are shown from figure 2.7 to 2.10.

Relative Humidity It is possible to observe how for both groups of tests, 20 and 30°C, increasing the speed of the fan a faster reduction of relative humidity entering in the HX is experienced. This implies that a much smaller difference between R_{in} and R_{out} is found for higher flow rates. The curve of the entering, and consequently the exiting flow, shows in general a behaviour similar to an exponential curve. As to say that, in the first hours, the variation is bigger and infact it corresponds to the time when the adsorption bed still have a high amount of moisture inside. Another remark can be made considering that the relative humidity exiting the heat exchanger is lower than the entering one, this is due to the fact that the temperature is increasing during the transformation. We are moving along the transformation 3-1 of figure 2.2

Temperature The stream temperatures entering and exiting the HX-ADS are almost constant, showing a constant difference. It is possible to make a further remark about a slight increase in temperature once the curves of relative humidity tend to stabilize, this correspond to a reduction in the condensed water from the air stream. It is worth to notice that for the tests done at $T_{amb} = 30C$, the sensor that measured the T_{in} got broken as it dumps continuously, so we cannot trust the results given by temperature and consequently the absolute humidity. This fail in the measure will have an impact for all the rest of measurements, they are not reliable.

Absolute Humidity The absolute humidity calculated as:

$$x = 0.622 \frac{RH \cdot p_{sat}(T)}{p_{tot} - RH \cdot p_{sat}(T)} \quad (2.3)$$

where p_{tot} is the ambient pressure set at 101325 Pa and p_{sat} is calculated in function of T as:

$$p_{sat} = exp\left(\frac{A \cdot T}{B + T} + C\right) \quad (2.4)$$

being A=17.438, B=239.78 and C=6.4147.

The curves starting from a large difference tend to come together as the number of

hours of the process gets sufficiently high.

Mass balance A further analysis can be made considering the mass balance in the HX-ADS. On the graph the quantity of water released during the regeneration process is displayed. The regenerated mass was calculated in 3 different ways:

- the first one was obtained considering the variation in weight measured by the load cell:

$$mr_{i+1} = ml_1 - ml_{i+1} \quad (2.5)$$

being mr_i the mass released at time $i+1$, ml_1 the mass measured by the load cell at the beginning of the test and ml_{i+1} the mass measured by the load cell at time $i+1$.

- the second way was obtained calculating the water released at each time step as:

$$dm = ((\rho_{out}(i+1) \cdot x_{out}(i+1) - \rho_{in}(i+1) \cdot x_{in}(i+1)) \cdot Q \cdot dt \quad (2.6)$$

and so the total mass

$$mr_{i+1} = mr_i + dm \quad (2.7)$$

being Q the mass air flow calculated according to the regulation of the fan using equation 2.1 and dt the time interval between the two measurements. The air densities in and out are calculated using the ideal gas law at the respective temperatures.

- the third way used is similar to the second one except that an average density was used:

$$dm = (x_{out}(i+1) - x_{in}(i+1)) \cdot \rho_{ave} \cdot Q \cdot dt \quad (2.8)$$

ρ_{ave} is calculated in function of an average temperature between the inlet flow and the outlet flow.

Specific Consumption A useful comparison among the different fan regulations, can be made calculating the specific consumption of the process at each time step. This is generally used to get an idea about the water produced in relation to the energy consumed. As we had the chance to see from previous analysis a faster regulation seems to lead to a better process. This aspect has to deal with the energy consumption associated to each regulation and can be used to find a trade off between the optimization of the specific consumption and the performances of the process.

The specific consumption is defined as:

$$e = \frac{P_{th} + P_{el-prim}}{Q(\rho_{out}x_{out} - \rho_{in}x_{in})} \left[\frac{kWh}{kg_{H_2O}} \right] \quad (2.9)$$

at the denominator all the quantities are referred to the air stream entering and exiting the regeneration battery.

P_{th} is the thermal power absorbed by the prototype from the boiler, it was calculated as:

$$P_{th} = \dot{m}_w c p_w (T_{in} - T_{out})_{prim} [kW]; \quad (2.10)$$

The electrical power consumed by the fan $P_{el-prim}$ had to be converted into primary source of energy before being used in the previous equation. It is firstly calculated considering the nominal power of the fan P_n and the regulation percentage FR as:

$$P_{el} = P_n \cdot FR; \quad (2.11)$$

and then according to the Authority for electric energy and gas (Autorità per l'energia elettrica e il gas) with "Delibera EEN 3/08[2] del 20-03-2008 (GU n. 100 del 29.4.08 - SO n.107)", the conversion factor from electricity to primary energy is fixed at $0.187 \cdot 10^{-3} tep/kWh$. Being 1 tep corresponding to 41.860 GJ, the final value is obtained as:

$$P_{el-prim} = P_{el} \cdot 0.187 \cdot 10^{-6} \cdot 41.860 \cdot 10^9 \quad (2.12)$$

Unfortunately, after this analysis it was not possible to compare the different regulations since they showed significantly different behaviours for the two groups of tests. The specific consumption tends to be very unstable after some hours of test, when x_{in} and x_{out} converge. It raises very rapidly as we can see for *fan70* at 20°C. However the tendency is to have less consumption for tests at higher fan speeds, this depends on

the fact that the electrical energy consumed is very small compared to the thermal one.

Dew Point Temperature The dew point temperature is a parameter that can be useful to identify the status of the air stream that has to be consensed. It is defined as the temperature to which air must be cooled to become saturated with water vapor. Analytically, the dew point temperature of a generic point in the psychrometric chart is obtained moving on a transformation with constant absolute humidity up to the saturation curve.

There exists some relation to calculate it in function of the saturation pressure as:

$$T_{dewpoint} = \frac{B \cdot (\log(p_{sat}) - C)}{A + C - \log(p_{sat})} \quad (2.13)$$

where p_{sat} is calculated as:

$$p_{sat}(\varphi = 1) = \frac{x_{out} \cdot p_{amb}}{(0.622 + x_{out}) \cdot 1} \quad (2.14)$$

It can be useful to compare it with ambient temperature since it is the temperature at which the condenser operates to produce the water and so the difference between the dew point temperature and the ambient temperature will be the driving force of the process. After the point where the two curves meet it is no more possible to perform the condensation. It is possible to see how this point is variable from test to test, generally test at lower temperatures tend to show this meeting point after more time than tests at higher temperatures, this is why for this particular aspect it may be more favorable to work in a cooler climate.

2.2.2 Adsorption

Regarding the adsorption process, a less accurate analysis was performed since the tests where all conducted under similar conditions and the tests showed similar behaviours between one test and the other. Five tests are reported in figure, plotting air and water temperatures.

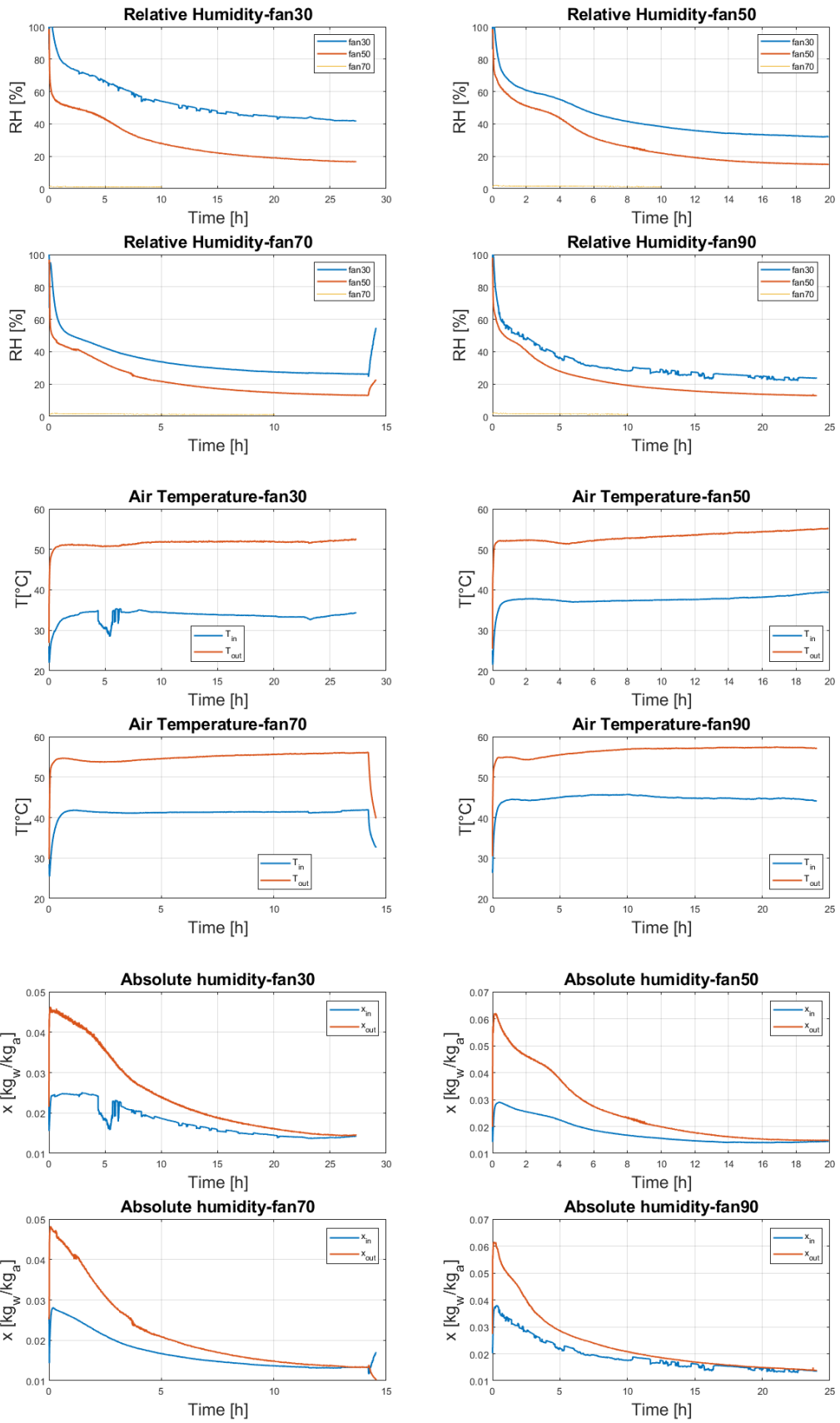


Figure 2.7: RH, temperature and absolute humidity for 20°C group of tests

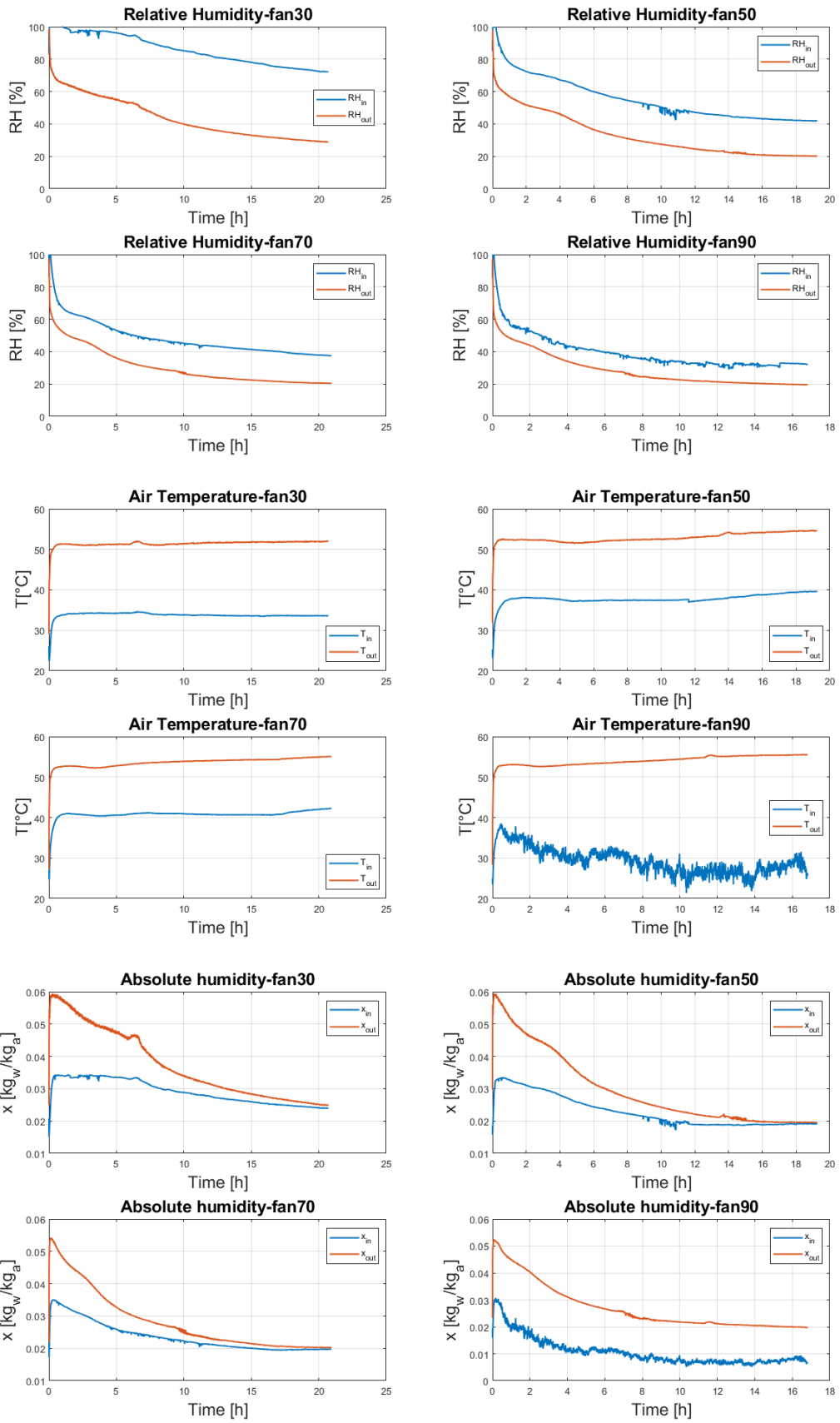


Figure 2.8: RH, temperature and absolute humidity for 30°C group of tests

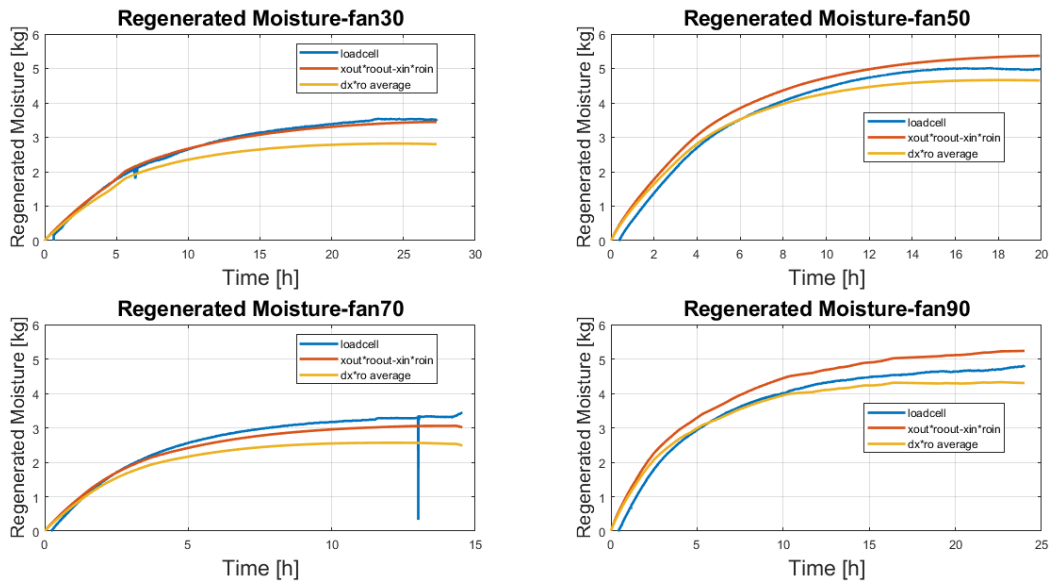


Figure 2.9: Mass released during the regeneration process for tests at 20°C

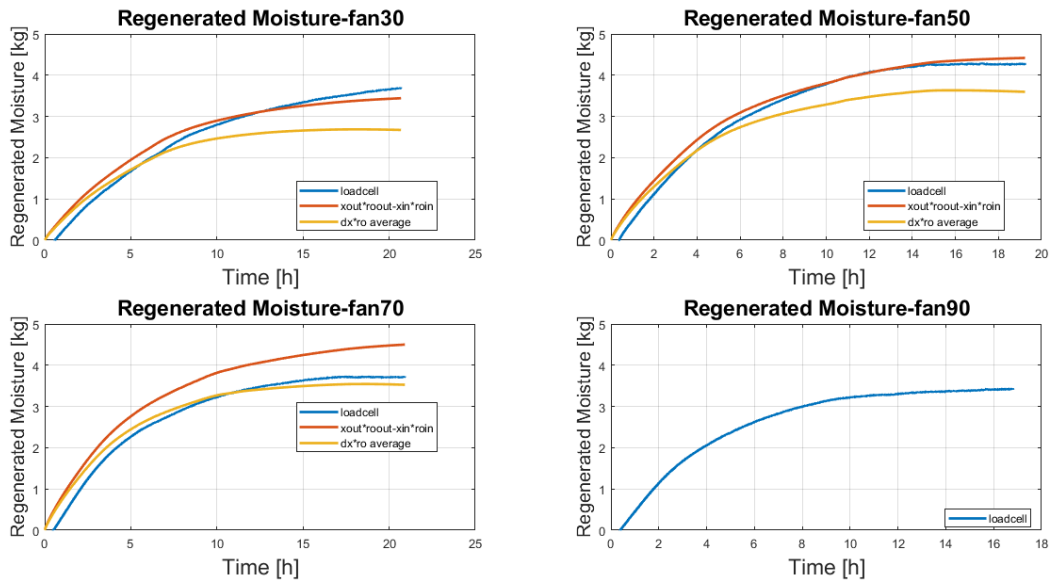


Figure 2.10: Mass released during the regeneration process for tests at 30°C

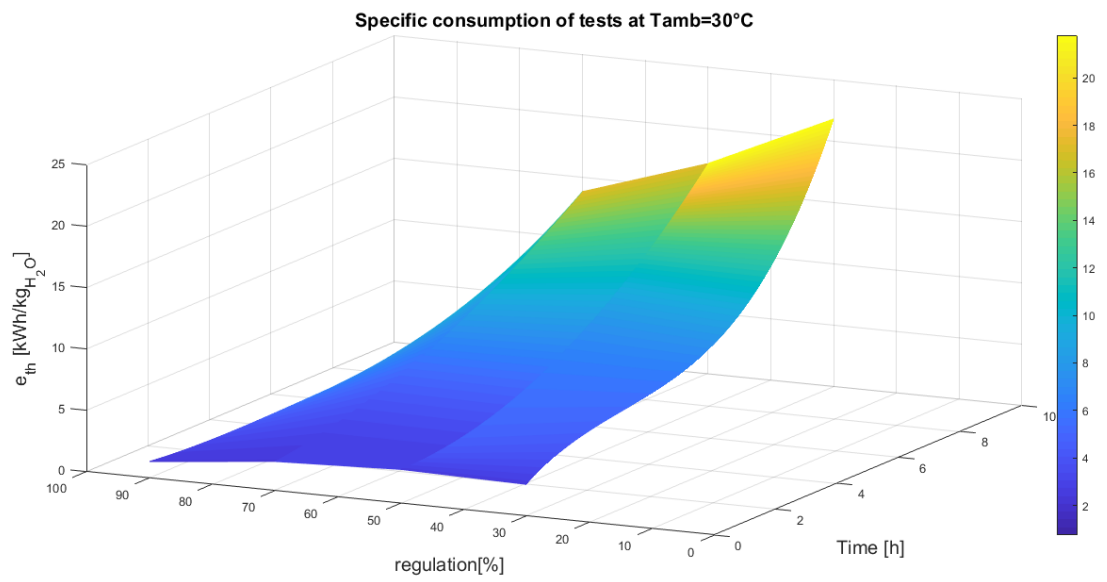
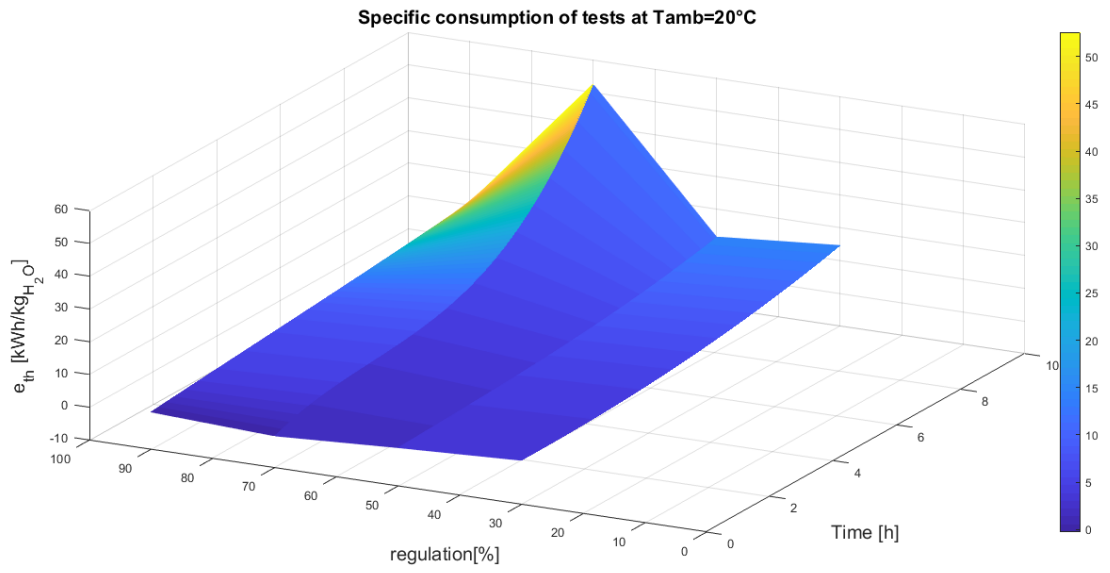


Figure 2.11: Specific consumption at different fan regulations

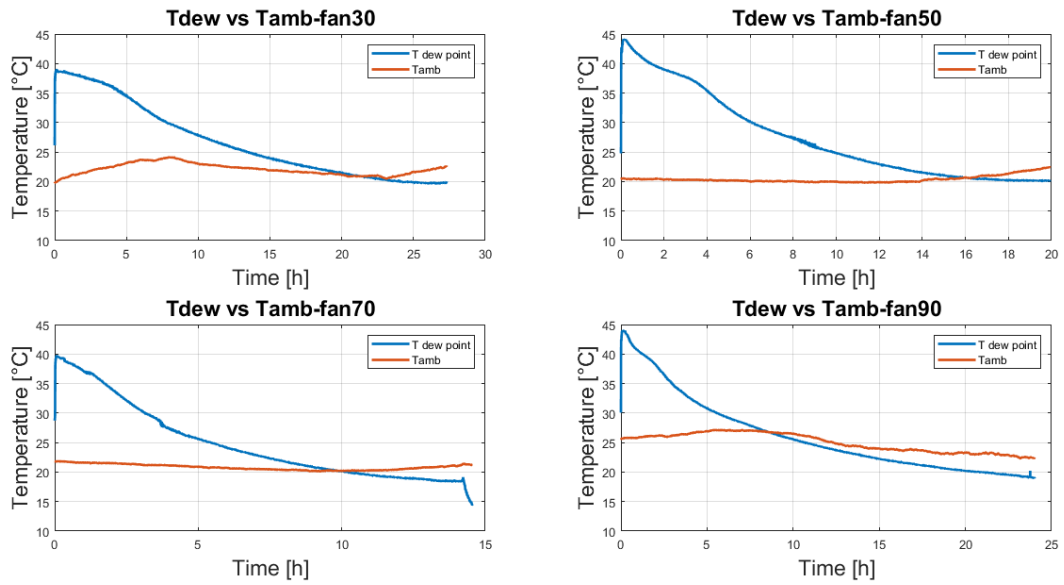


Figure 2.12: T dew point vs T amb for tests at 20°C

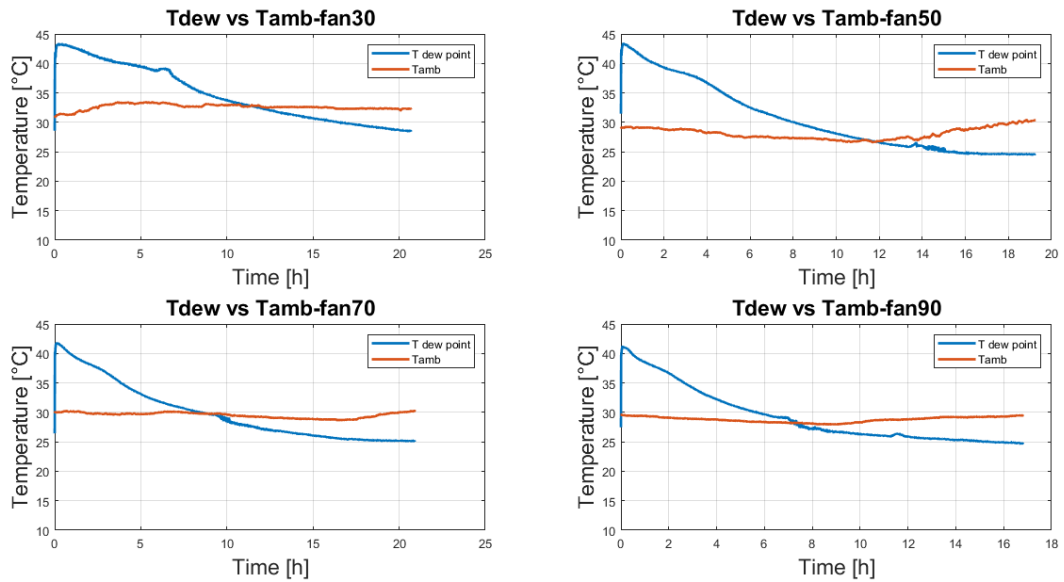


Figure 2.13: T dew point vs T amb for tests at 30°C

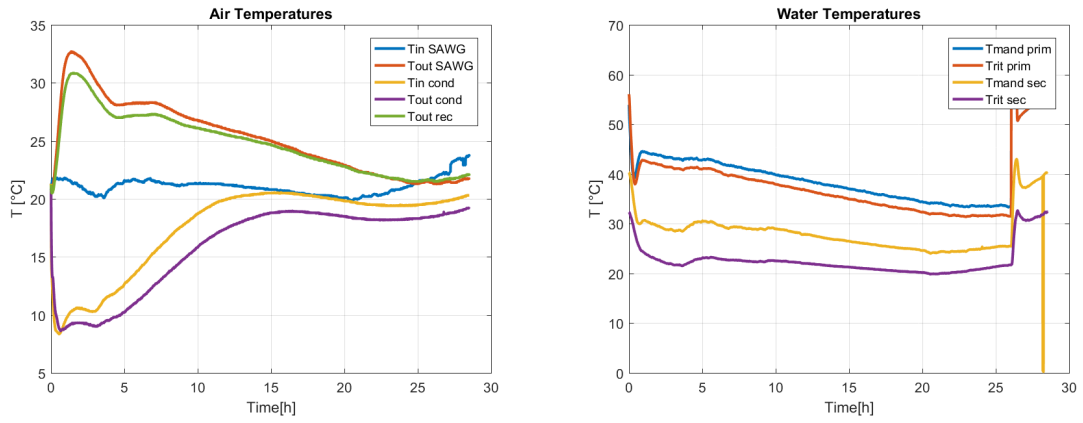


Figure 2.14: TEST 20-ADSORPTION

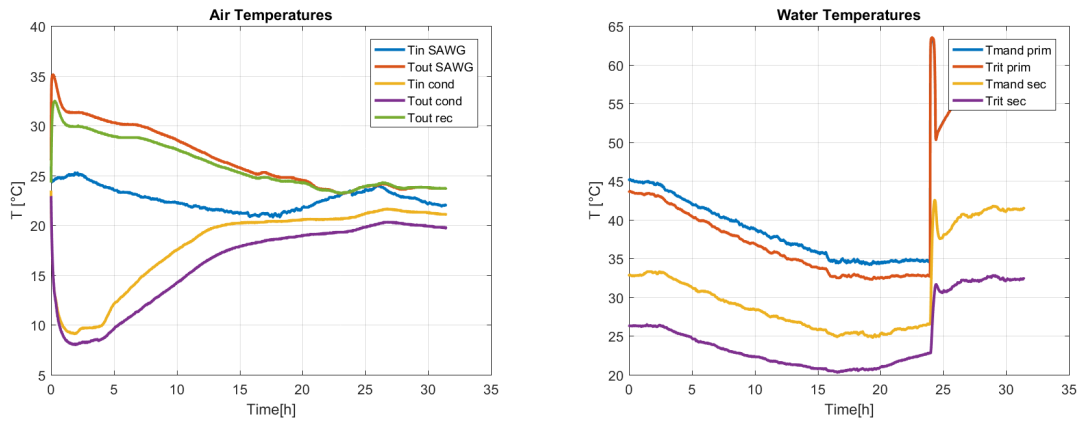


Figure 2.15: TEST 22-ADSORPTION

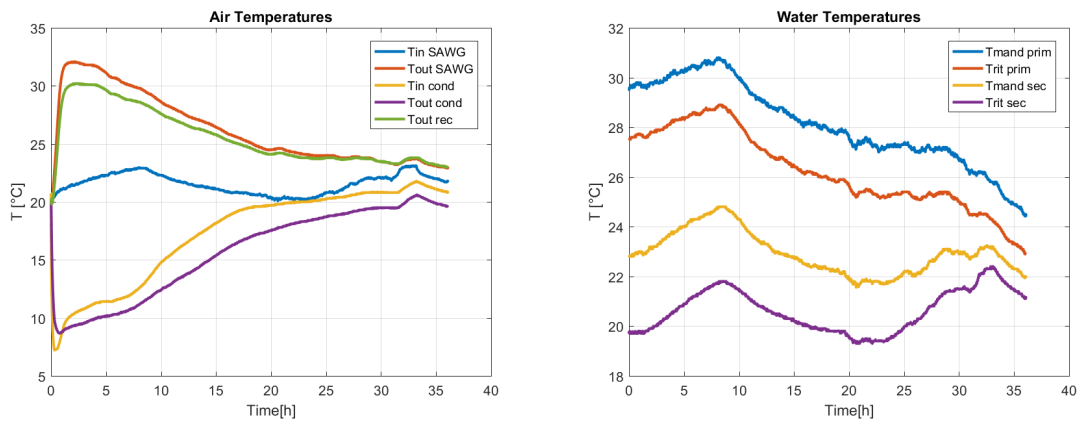


Figure 2.16: TEST 26-ADSORPTION

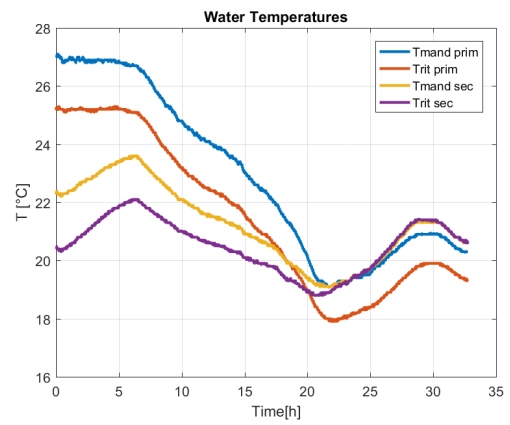
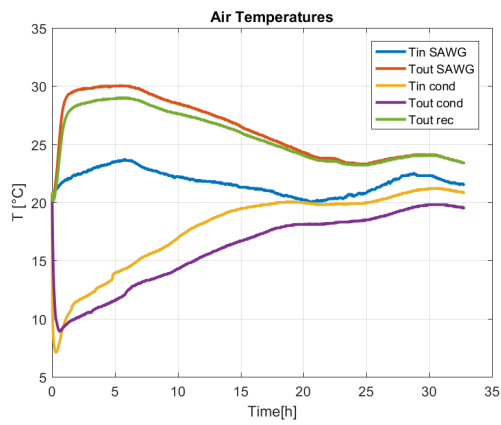


Figure 2.17: TEST 28-ADSORPTION

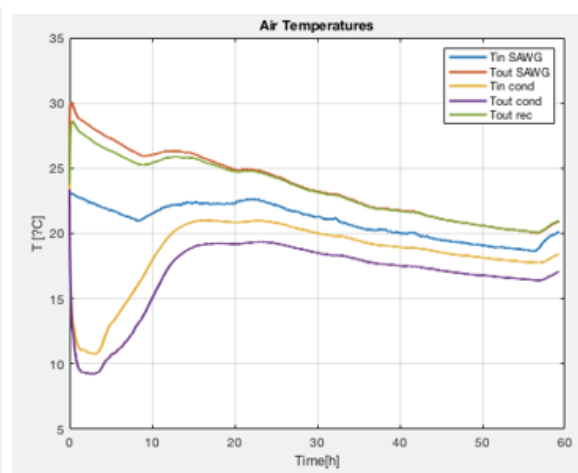
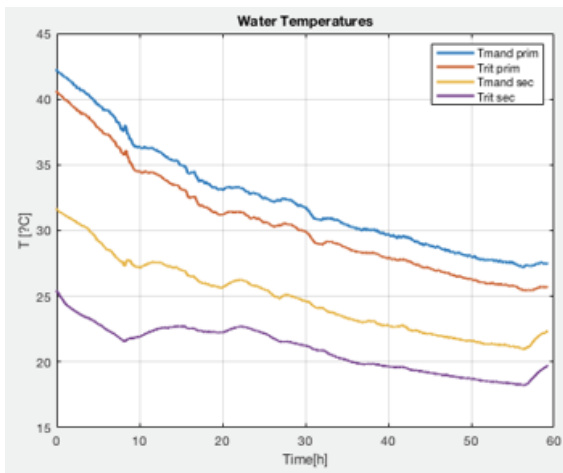


Figure 2.18: TEST 32-ADSORPTION

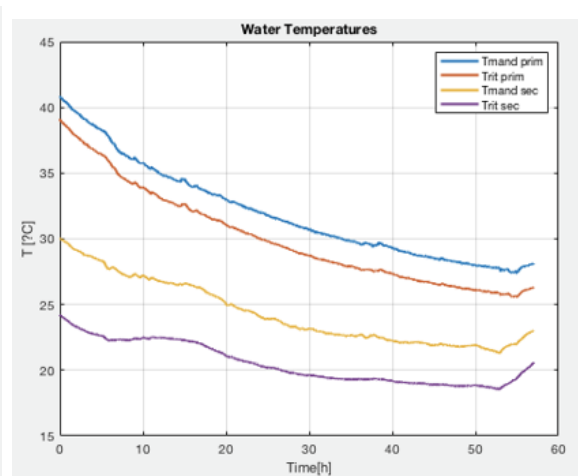
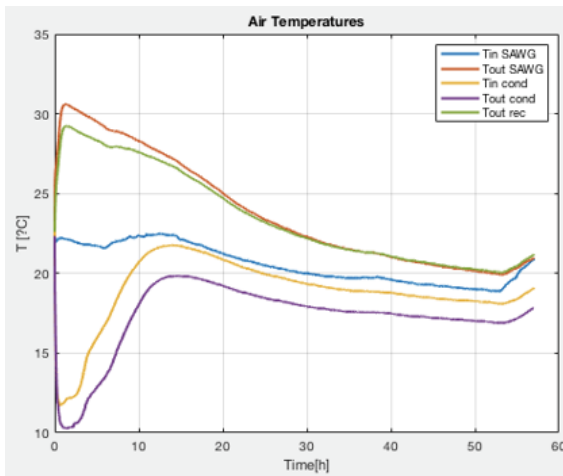


Figure 2.19: TEST 38-ADSORPTION

Chapter 3

SAWG prototype

This work had the aim to contribute to the realization of the SAWG (Solar Atmospheric Water Prototype) that could work in real atmospheric condition, in particular arid climates. It has been funded by the interdepartmental center Clean Water Center and was assembled in the laboratory of Energy Department (DENERG) of Politecnico di Torino. It is coupled with two solar flat plate collector, that are meant to supply the thermal energy needed by the prototype. It was designed in such a way that it is more compact and can be easily moved. The whole system is contained in a cube of few more than a meter per side and the structure to support the two solar collectors.

The working principle of this prototype is the same of the test prototype with the difference that this one has 2 HX-ADS. They work alternatively in such way that when one is performing regeneration, the other is doing adsorption. The idea was to optimize this process of switching between the two batteries when it is more convenient in terms of efficiency.

3.1 Components description

A functional scheme of the prototype is given in figure 3.6. In the scheme we can distinguish the air circuits and the water circuits.

The water circuits are two:

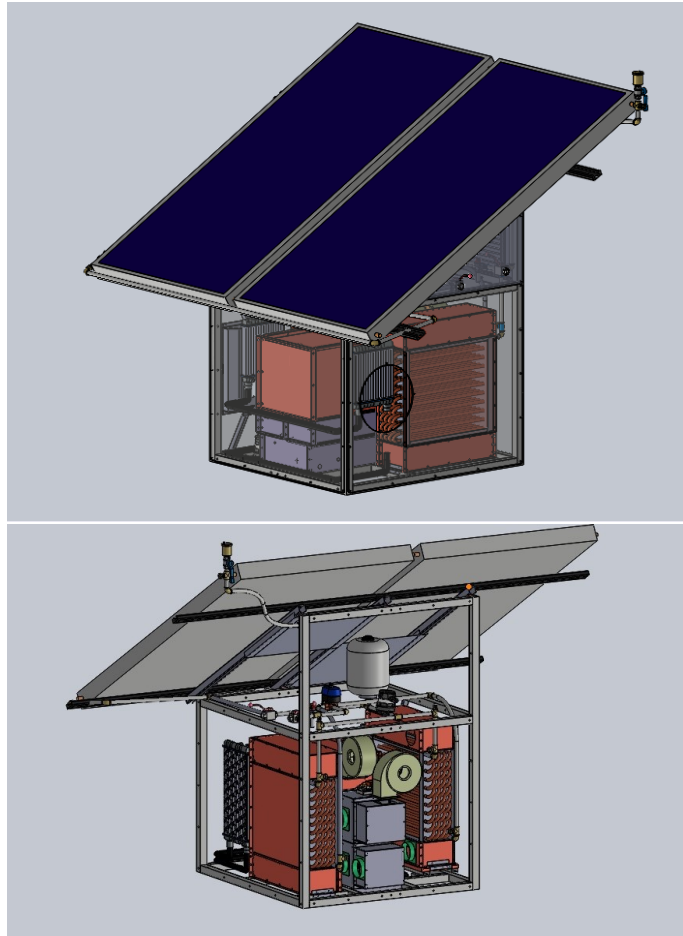


Figure 3.1: SAWG 3D

- the solar circuit: is the one delivering the heat needed for the regeneration process, the direction of the hot flux is decided by a motorized valve;
- the condenser circuit: is a closed loop used by the condenser to extract heat and deliver it to the outside.

The air circuits are connected to a 4-way valve that can alternatively address the air to the regeneration closed loop or adsorption loop. A brief overview of the components of the prototype will be given.

Solar Collectors The solar collectors are two flat plate collectors of $2m^2$ of gross area each, with dimensions: $1980 \times 1010mm$. The installed idraulic configuration permits to use them both in series or in parallel. They are installed on the prototype with a tilt angle of 30° .

Batteries The two batteries installed are conventional batteries filled with silica gel spheres of 3 mm of diameter. The amount of silica gel putted inside is 18.77 kg. Each battery is $630 \times 485 \times 190 \text{ mm}$ and they are installed symmetrically one on the left and the other on the right side.

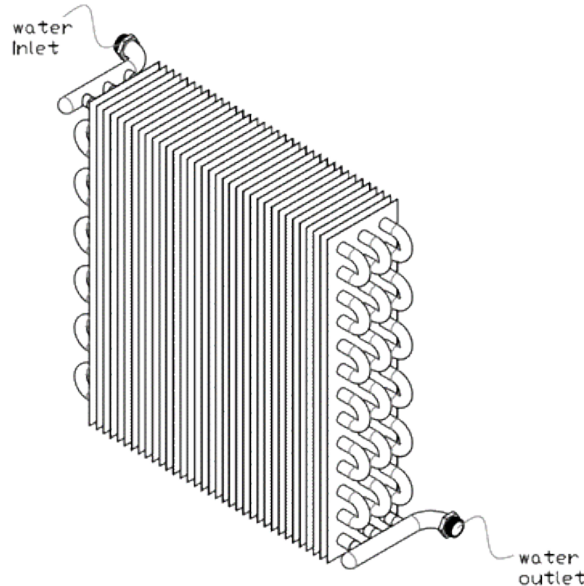


Figure 3.2: Adsorption battery

Condenser The condenser unit is composed of two parts: in the upper part we find a heat exchanger encharged of cooling down the air going successively to the proper condenser and at the same time pre-heat the air exiting the condenser. This component is connected to the battery that is performing the regeneration.

In the lower part the proper condenser is found, it is connected to the external environment through a radiator connected to the condenser water circuit. The water is sent to two other radiators, the flux is splitted, placed in the external position and encharged of exchanging heat with the ambient air. The heat exchange is enhanced by two fans, placed right in front of both the radiators.

Double four-way valve This component is a double valve that is able to switch the air fluxes in order to change the function of the ADS-HX from adsorption to

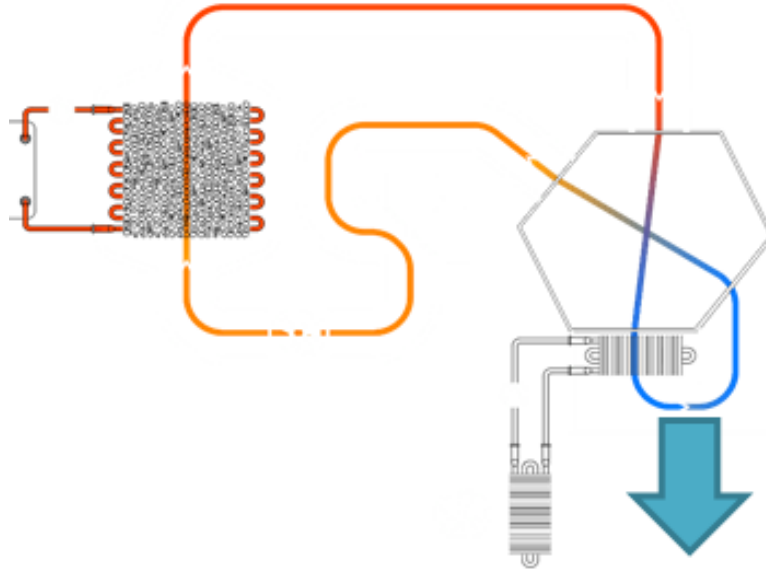


Figure 3.3: Condenser + regeneration air circuit

regeneration and viceversa. It is moved by an actuator placed on top of it that moves the inner shaft.



Figure 3.4: Double four-way valve before being installed

Fans Two bigger fans are used in the prototype to move the air of the regeneration and adsorption circuit. They have a maximum nominal power of 65W, the fan attached to the regeneration circuit has the possibility to be regulated. The other two fan present in the circuit are the ones connected to the radiators that goes to the condenser circuit. They have a maximum rated power of 170W.

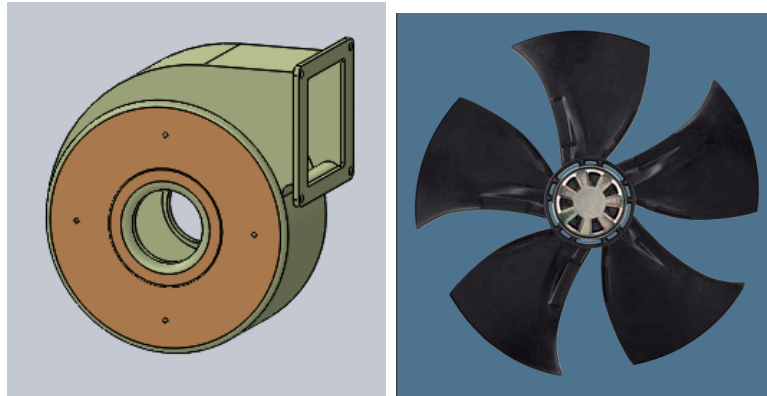


Figure 3.5: On the left RIG/ADS fans, on the right condenser circuit fans

Sensors As visible from the functional scheme, two types of sensors are installed in the prototype: the temperature ones and the relative humidity ones.

Concerning the temperature sensors, the LM35 precision centigrade Temperature Sensors have been used. They are precision integrated-circuit temperature sensors, whose output voltage is linearly proportional to the temperature. They have an accuracy of $\pm 1/4^{\circ}\text{C}$ at room temperature and $\pm 3/4^{\circ}\text{C}$ over a full -55 to $+150^{\circ}\text{C}$ temperature range. It can be used with single power supplies, or with plus and minus supplies. As it draws only $60 \mu\text{A}$ from its supply, it has very low self-heating, less than 0.1°C in still air.

The moisture sensors used are the HIH-4000 Series Humidity Sensors. The sensor's near linear voltage output makes the direct input to the controller. They work with a typical current draw of $200 \mu\text{A}$. They have an accuracy of $\pm 3.5\%$.

Both types of sensors give to the controller unit an analogic input. A list of all the installed sensors is given in table below.

Name	Fluid	Type	Location
TBD1	Air	Temperature	Inlet HX-ADS-DX
TBD2	Air	Temperature	Outlet HX-ADS-DX
TBS1	Air	Temperature	Inlet HX-ADS-SX
TBS2	Air	Temperature	Outlet HX-ADS-SX
TBD3	Water	Temperature	Inlet HX-ADS-DX
TBD4	Water	Temperature	Outlet HX-ADS-DX
TBS3	Water	Temperature	Inlet HX-ADS-SX
TBS4	Water	Temperature	Outlet HX-ADS-SX
TC1	Air	Temperature	Inlet Condenser
TC2	Air	Temperature	Outlet Condenser
TC3	Water	Temperature	Inlet Condenser
TC4	Water	Temperature	Outlet Condenser
TPD	Water	Temperature	Outlet Solar Collector-DX
TPS	Water	Temperature	Outlet Solar Collector-SX
FP	Water	Mass Flow	Solar circuit
RHBD1	Air	Relative Humidity	Inlet HX-ADS-DX
RHBD2	Air	Relative Humidity	Outlet HX-ADS-DX
RHBS3	Air	Relative Humidity	Inlet HX-ADS-SX
RHBS4	Air	Relative Humidity	Outlet HX-ADS-SX

Table 3.1: List of sensors

Controllino This unit is the controller, it is able to read analogical input coming from the circuit, elaborate them and send an analogic or digital output to the components. A controller logic could be implemented in order to optimize the performances of the prototype with the variation of external conditions.

Load cell Under one of the two batteries a load cell is placed, with the aim to detect the weight variation of the HX and so the water adsorbed or released. It is used as a double check with the RH and T sensors.

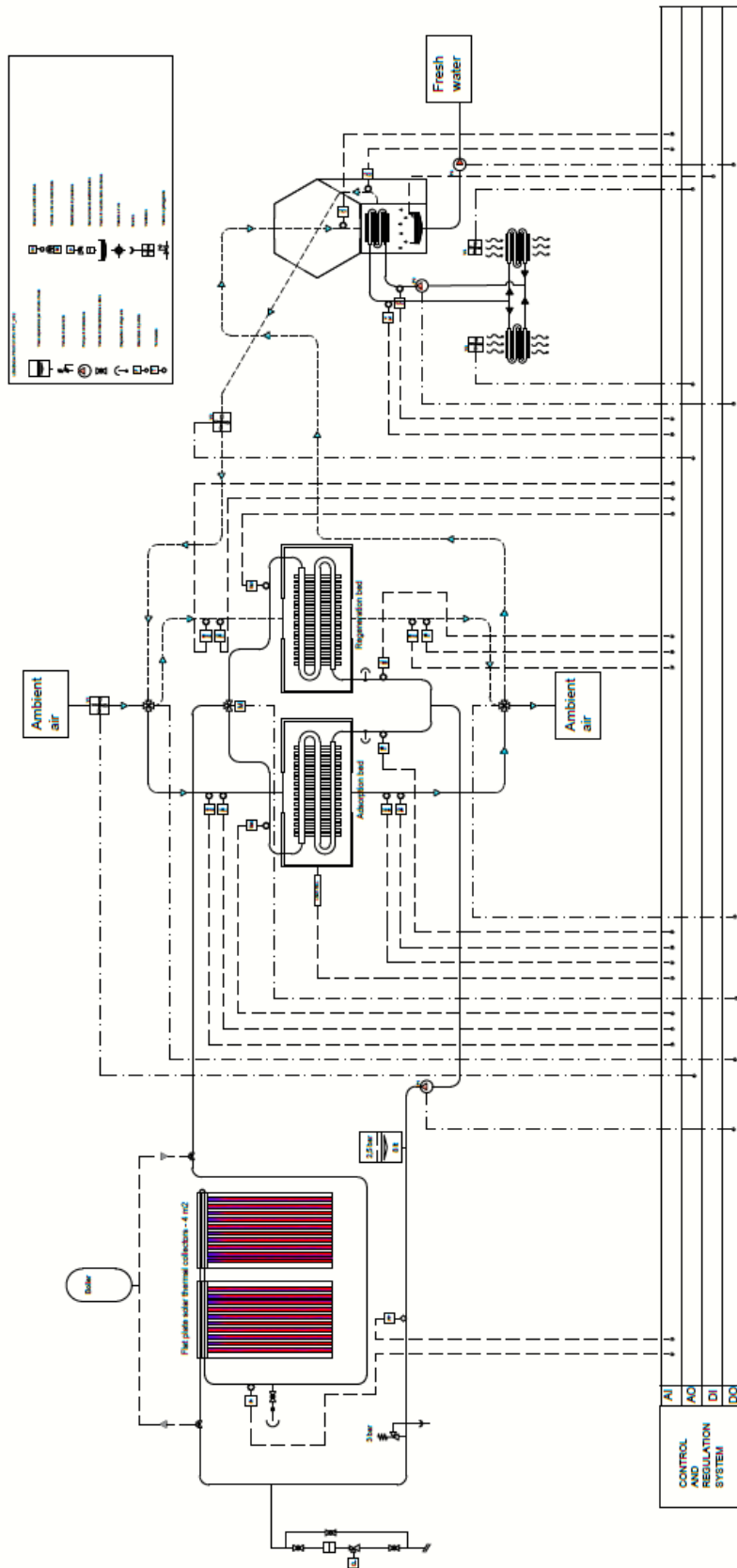


Figure 3.6: Functional scheme



Figure 3.7: Assembled prototype

Chapter 4

Model description

4.1 TRNSYS model

In order to investigate the behaviour of the prototype in different climatic conditions, a simulation model was developed on the software TRNSYS. In this model, many of the components of the existing prototype are present but some of them are simplified. For most of them, it already existed a correspondent component inside the software libraries, but for the adsorption/desorption bed a Matlab model that is explained in detail in the next paragraph, has been used.

Further on, each block of the model will be analyzed in detail.

PUMP It represents the pump of the solar circuit. This component sets the flow rate for the rest of the components in the flow loop by multiplying the maximum flowrate by the control signal. It is connected to a hourly controller that according to the user regulation is able to turn the pump on or off. As a first approach it was supposed to have it on between 8am and 6pm assuming to use all the solar energy for the regeneration processes.

The parameter needed by this component are given in table 4.1

The conversion coefficient mentioned in the table, is referred to the fraction of pump power that is converted to fluid thermal energy. It can be defined as:

$$f = \frac{Power}{\dot{m}c_p(T_{out} - T_{in})} \quad (4.1)$$

Parameter	Unit	
Maximum flow rate	50	kg/h
Fluid Specific Heat	4.186	KJ/kgK
Maximum power	60	kg/h
Conversion coefficient	0.05	-
Power coefficient	0.5	-

Table 4.1: Pump parameters

where the power refers to the power actually consumed by the pump.

On the other hand, the power coefficient is introduced to specify a non-linear relationship between pump power and fluid flow rate. This relation is expressed by:

$$Power = P_{max}^*(c_0 + c_1^*\gamma + c_2^*\gamma^2 + c_3^*\gamma^3 + c_i * \gamma^i) \quad (4.2)$$

where the P_{max} is the maximum power found among the parameters, γ is the input control signal between 0 and 1, $c_0...c_i$ are the coefficients relating power to the flow rate. In this case only the first coefficient was set.

The inputs of this component are given in table below:

Input	Unit
Inlet fluid temperature	°C
Inlet mass flowrate	kg/h
Control signal	-

Table 4.2: Pump inputs

The outputs of the component are: the outlet fluid temperature [°C], the outlet flowrate [kg/h] and the power consumption [kJ/h] calculated using equation 4.2.

PANELS This component models the thermal performance of a flat-plate solar collector. The two panels were modelled using data coming from the datasheet of the panels used in the laboratory. (The factsheet can be found in the Appendix). The

parameters that were implemented for each panel are listed below:

Parameter		Unit
Collector area	2	m^2
Fluid Specific Heat	4.186	KJ/kgK
Tested flowrate	72	$kg/(hrm^2)$
a_0	0.788	-
a_1	5.140	$W/(m^2K)$
a_2	0.017	$W/(m^2K^2)$

Table 4.3: Collectors parameters

The coefficients a_0 , a_1 and a_2 comes from the definition of the panel efficiency as:

$$\eta = a_0 - a_1 \frac{(T_{in} - T_{amb})}{G} - a_2 \frac{(T_{in} - T_{amb})^2}{G} \quad (4.3)$$

being G the incident radiation on the panel.

This component is also linked to the external weather condition file that provides all the information about ambient condition. Depending on the latitude and the climatic zone the performance of this component will visibly change. It was possible to load different files from different locations and check this behaviour. In particular the input parameter required by the panel TRNSYS model were:

Both the inlet temperature and inlet flowrate are datas coming from the previous component, the pump. The collector slope was set 30° , the other parameters changes during the day and the year.

The output data coming from the panel are: the outlet temperature [$^\circ\text{C}$], the outlet flowrate [$^\circ\text{C}$] and the useful energy gain [kJ/h]. This last parameter was is calculated as:

$$Q_u = \dot{m}c_p(T_{out} - T_{in}) \quad (4.4)$$

Since in the prototype 2 panels were installed, this situation was represented connecting in series these components in the model. This implies that the outlet temperature of the first one is the inlet temperature of the second one; the same happens for the flowrate that is the same flowing in the two panels.

Parameter	Unit
Inlet temperature	°C
Inlet flowrate	kg/h
Ambient temperature	°C
Incident radiation	KJ/m^2h
Total horizontal radiation	KJ/m^2h
Ground reflectance	-
Incidence angle	°
Collector slope	°

Table 4.4: Collector inputs

HX-ADS This is the block that recalls the matlab routine that is explained in detail in section 4.2. It simulates the behaviour of the adsorption/regeneration heat exchanger filled with silicagel, for each step of the simulation it communicates with TRNSYS which gives to it 8 inputs and receives 6 outputs.

The inputs are:

- T_{w-in} is the temperature of the water exiting the panels and entering the heat exchanger;
- \dot{m}_w is the water flowrate exiting the panels and entering the heat exchanger;
- T_{air-in} is the temperature of the air entering the heat exchanger. Depending on what process the system is performing it is equal to the ambient temperature in case of adsorption, and equal to 40°C if the system is performing regeneration. The value chosen for regeneration, was obtained from the data analysis on the test bench prototype, it was seen that the temperature is almost constant in regeneration phase and for each fan regulation is around the value of 40°C;
- x_{air-in} is the absolute humidity of the air entering the heat exchanger. It is set equal to the ambient absolute humidity if the system is performing the adsorption, on the other hand, if the system is doing regeneration it is set to a constant

value calculated in function of T_{air-in} and $RH = 0.9$. This value corresponds to the condition of the air entering the heat exchanger after being condensated, from the experimental data it was not properly constant, but in this case it is set as constant as a simplification;

- w_{in} is the relative water content of the bed [kg_w/kg_s]. Through the TRNSYS type 661, the values for each iteration are updated with the final value of the previous iteration, after setting an initial value. Since the model divides the bed in 18 layers and has as output 18 values of w for each layer, as a simplification a mean value among them is used and reassigned in the next iteration;
- T_{s-in} is the bed temperature. As for the water content, the TRNSYS type 661 is used so the values are updated with the output values of the previous iteration. Again, since the model divides the bed in 18 layers and has as output 18 values of w for each layer, as a simplification a mean value among them is used and reassigned in the next iteration;
- E is the effectiveness of the heat exchanger, set to 0 for adsorption and 0.5 for regeneration;
- \dot{m}_a is the air flow rate, set to $200m^3/h$ for adsorption and $45m^3/h$ for regeneration.

Inside the script there are also the inputs needed by the model to perform the calculation, but they are not reported nor saved on TRNSYS since they are constant in time and not needed for the simulation purpose.

The output of the model are:

- T_{w-out} the temperature of the water exiting the heat exchanger and sent back to the inlet of the collectors, passing through the pump;
- $T_{air-out}$ the temperature of the air exiting the heat exchanger;
- $x_{air-out}$ the absolute humidity of the air exiting the heat exchanger;
- w_{out} the relative water content of each layer of the bed;

- T_{s-out} the temperature of each layer of the bed;
- $T_{dewpoint}$ calculated within the matlab routine in function of the vapor pressure. This temperature is a fundamental parameter for the regeneration phase, since it has to be higher than the ambient temperature in order to make the condensation possible.

The HX-ADS is connected to a series of equation that regulate the switch among the regeneration and the adsorption processes. The switch is performed considering the temperature exiting the panels. If it is sufficiently high ($T_w > 50C$) calculator sets all the parameters for regeneration. On the other hand, if it $T_w < 50C$ the adsorption is performed.

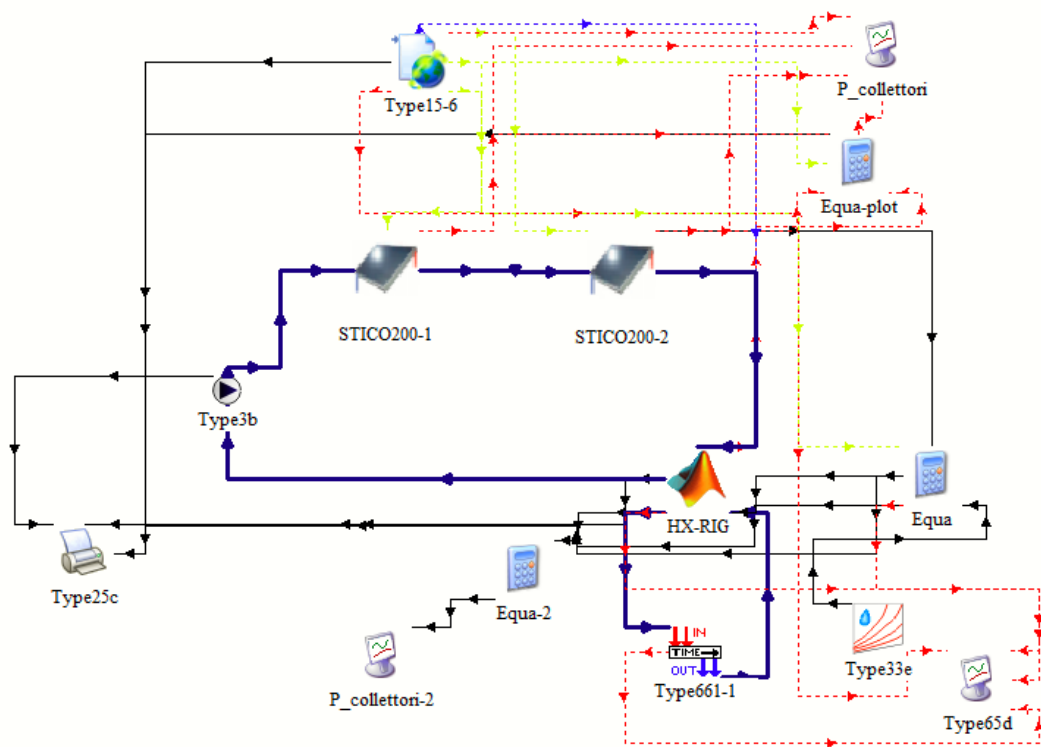


Figure 4.1: TRNSYS model scheme

4.2 Matlab routine

The model developed on Matlab has the aim of simulating the behaviour of the HX-ADS, being a heat and mass exchanger.

In adsorption/desorption processes, it exists a strong correlation between mass and heat transfer due heat of adsorption/desorption that is released or absorbed by packed bed. This model is focused on the study of the packed bed filled with adsorbent material, air can flow through the bed lapping sorbent material, and finally adsorption or desorption phenomena will happen depending by inlet air and sorbent humidity conditions.

We start with the hypotesis that the bed is composed by pseudospherical particles of silica gel with an average diameter $D=3\text{mm}$, uniform initial temperature T_0 and humidity content W_0 . The air stream flows directly through the bed with temperature and moisture conditions T_{airin} and x_{airin} respectively. A water vapour mass transfer happens between air and sorbent particles.

To evaluate the air humidity of the layer near particles, adsorption isotherms of the material are needed.

The hypotesis of the model are listed below:

1. Physical adsorption and desorption are much faster than other phenomena like water vapour diffusion through capillary of sorbent material. So in the neighbouring area a local and instantaneous equilibrium condition exists;
2. All the problem can be simplified in one dimension, the only direction analyzed is along air flow, that will be supposed stationary;
3. Adsorption heat due to “condensation” of water vapour is directly generated in the pore volumes;
4. The heat is transferred by air forced convection. Heat conduction between sorbent material can be neglected in all the direction, in particular along flow direction, hence temperature gradient it's only function of convection phenomena;
5. Pressure drops are little if compared with total ambient pressure (atmospheric

pressure), so hypothesis of constant pressure it's assumed, and it will be equal to atmospheric pressure 101325 Pa.

4.2.1 Silica-gel isotherm adsorption curves

In order to model the behaviour of the silica gel, its characteristic isotherm curves are needed. Isotherm curves permit to evaluate air bulk relative humidity (RH), as a function of the moisture content of the adsorption material $w[kg_{water}/kg_{silica}]$ and the temperature of silica gel $T [^{\circ}C]$. In a previous work, these curves relative to the silica gel used in the bench prototype were obtained in the laboratory. A sample of adsorption material grains was weighted changing the variables RH and T. The experiment were conducted in a climatic room, that permitted to maintain the temperature constant during the experiment.

After collecting the experimental data, it was possible to obtain the following regression that correlates relative humidity with the water content and the temperature:

$$RH = S1 \cdot T + S2 \cdot T^2 + S3 \cdot w + S4 \cdot w \cdot T + S5 \cdot w \cdot T^2 + S6 \cdot w^2 + S7 \cdot T \cdot w^2 + S8 \cdot w^3 + S9 \cdot T^3 \quad (4.5)$$

In table 4.5, the values of the coefficients of equation 4.5.

S1	-0.00249434
S2	0.0000529632
S3	5.65527
S4	0.0360887
S5	-0.0000713679
S6	-24.9044
S7	-0.112424
S8	54.8088
S9	-0.000000123558

Table 4.5: Regression parameter values

Solving the equation between 20°C and 70°C we map some possible functioning condition of adsorption/desorption phenomena.

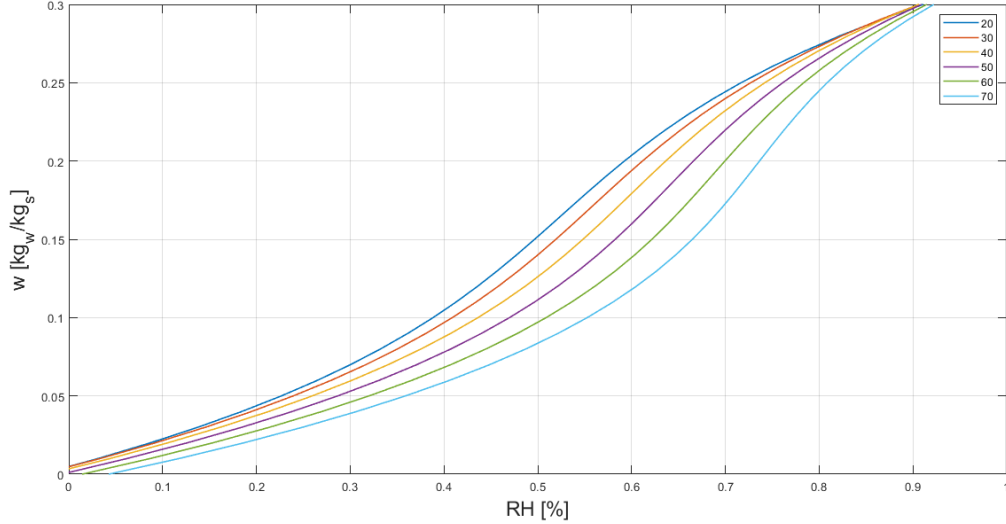


Figure 4.2: Isotherms of adsorption

We can observe how the temperature affects the behaviour of the bed at the equilibrium. For higher temperatures we get lower water content in the bed, and viceversa decreasing the temperature the water content is lower.

In order to simplify the model calculation, it was useful to rewrite the relation of the relative humidity in terms of absolute humidity. In this way we aim to obtain an equation with only two variable, being x a quantity that contain both the information of RH and T. This is possible through equation 4.6

$$x = \frac{0,622}{\frac{p_a}{p_{sat}(T) \cdot RH} - 1} \quad (4.6)$$

In this way we obtain a relation between absolute humidity and water content and a new family of curves is obtained.

It becomes now possible to express the absolute humidity in terms of w . A third order polynomial was needed to ensure the fitting of the curves. The new isotherms curves and their fittings are shown in figure 4.3.

$$x^* = k_1 \cdot w^3 + k_2 \cdot w^2 + k_3 \cdot w + k_4 \quad (4.7)$$

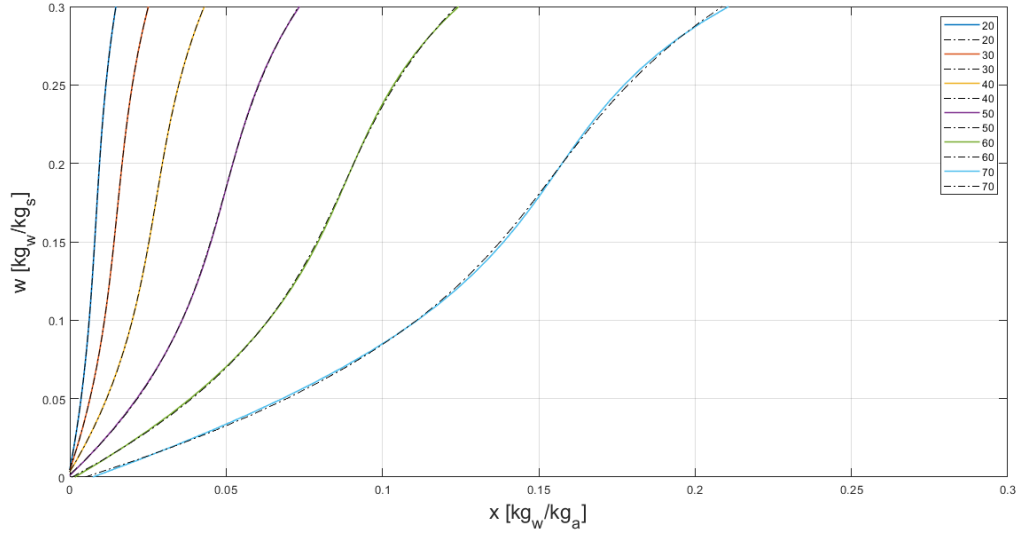


Figure 4.3: Isotherms of adsorption in function of absolute humidity

The symbol * stays for the equilibrium condition reached between the air stream and the adsorbent material particles. k_1 , k_2 , k_3 and k_4 are the constants depending on equilibrium temperature between sorbent and the fluid. Their values are shown in table 4.6.

T[°C]	k_1	k_2	k_3	k_4
20	0,8824	-0.4336	0.1014	-4.8252e-4
30	1.5003	-0.7646	0.1808	-8.5176e-4
40	2.5348	-1.3358	0.3195	-0.0011
50	4.2086	-2.2880	0.5545	-8.9969e-4
60	6.7996	-3.8098	0.9407	6.9795e-4
70	10.6860	6.1814	1.5719	0.0049

Table 4.6: Constant k_i values in function of temperature

In this way, it is possible to obtain a polynomial regression that approximates the value of k in function of temperature. A fourth degree polynomial was used, as visible in equation 4.8

$$k_i(T) = C_{1-i} \cdot T^4 + C_{2-i} \cdot T^3 + C_{3-i} \cdot T^2 + C_{4-i} \cdot T + C_{5-i} \quad (4.8)$$

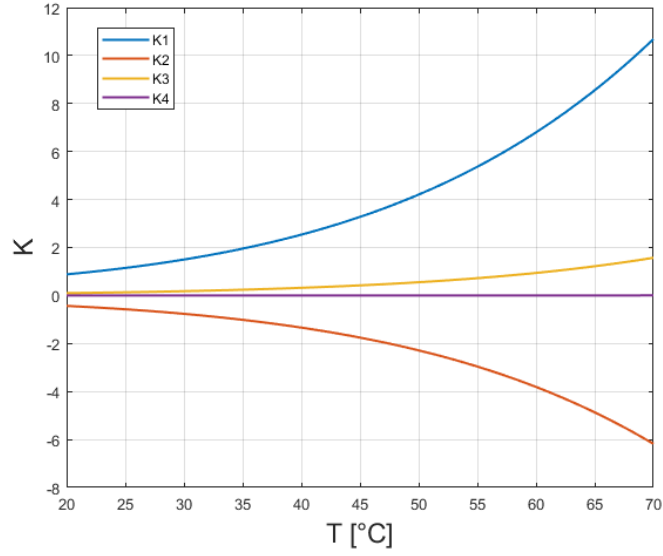


Figure 4.4: Temperature dependence of coefficients used for polynomial approximation of adsorption isotherms

The coefficients for each k are:

k	C_1	C_2	C_3	C_4	C_5
k_1	3.2432e-7	-9.9730e-6	0.0012	-0.0012	0.4491
k_2	-2.9056e-7	1.8844e-5	-0.0013	0.0160	-0.3303
k_3	1.1852e-7	-1.1206e-5	6.6180e-4	-0.0116	0.1396
k_4	1.6940e-9	-1.6466e-7	5.9290e-6	-1.3063e-4	8.0470e-4

Table 4.7: Constant k_i values in function of temperature

4.2.2 Model equations

The main equations used in the model can be subdivided in mass balance equations and thermal balance equations.

The mass balance used in the model is based on the hypothesis that the variation with respect to time of the water content in the bed is equal to the air stream flow multiplied by the difference of absolute humidity between the input and the output.

Analytically we have:

$$\frac{d(m_s W)}{dt} = \dot{m}_a(x_i - x_e) \quad (4.9)$$

where:

- m_s is the mass of the dry silica gel in the bed [kg];
- W is the relative water content in the bed [kg_w/kg_s];
- \dot{m}_a is the air flow rate [kg/s];
- x_i and x_e respectively the inlet and outlet absolute humidity of the air [kg_w/kg_a].

Regarding the thermal balance, according to the third hypothesis, heat is released or absorbed directly in the particle, this phenomenon will obviously cause the increasing or decreasing of bed temperature.

For solid phase we have:

$$h_{ads} M_t A(x_i - x_e^*) = H_t A_S(T_s - T_a) + (1 - \varepsilon)\rho_s c_s \frac{\delta T_s}{\delta t} \quad (4.10)$$

where H_t and M_t are respectively the heat and mass transfer coefficients, h_{ads} is the specific thermal power generated or absorbed during mass transfer process. If mass transfer goes from air to sorbent material, heat is generated; viceversa it will be absorbed.

For the gaseous phase no heat is produced, but heat is exchanged through convection along the flow direction.

$$C_a \rho_a \nu \frac{\delta T_a}{\delta x} = h A(T_s - T_a) \quad (4.11)$$

4.2.3 Model algorithm

The model algorithm is based on an iteration process that calculates the HX-ADS quantities at each subsequent timestep, imposing a $dt = 30s$. The bed is subdivided in 18 monodimensional layers from inlet to outlet and it is assumed that the outlet condition of layer n is the inlet condition for layer $n + 1$.

The algorithm with the calculation of T_{eq} in each layer, that is the temperature reached

by the air in the neighbourhood of the silica gel particles, assuming the air flow to reach the equilibrium condition in that area.

$$T_{eq} = T_s + (T_a - T_s) \cdot e^{-i} \quad (4.12)$$

where coefficient i is given by:

$$i = \frac{A_s \cdot H_t \cdot l}{v \cdot \rho \cdot c_a} \quad (4.13)$$

Once the equilibrium temperature is obtained, it is possible to obtain the constants of equation 4.8 so that:

$$k_i = k_i(T_{eq}) \quad (4.14)$$

At this point, the equilibrium water content is calculated in function of x_{in} . Among the roots of the polynomial, the only real solution is chosen.

$$k_1 w_{eq}^3 + k_2 w_{eq}^2 + k_3 w_{eq} + k_4 = x_{in} \quad (4.15)$$

It becomes now possible to solve the mass balance substituting x_{in} and x_{out} in function of the water content:

$$\frac{dw}{dt} = \frac{\dot{m}_a}{m_s} [k_1(w_{eq}^3 - w^3) + k_2(w_{eq}^2 - w^2) + k_3(w_{eq} - w)] \quad (4.16)$$

The equation cannot be solved analytically so a numerical method was implemented approximating as:

$$\frac{dw}{dt} \approx \frac{w_{i+1} - w_i}{dt} = \frac{\dot{m}_a}{m_s} [k_1(w_{eq}^3 - w_i^3) + k_2(w_{eq}^2 - w_i^2) + k_3(w_{eq} - w_i)] \quad (4.17)$$

$$x_{out} = x_{in} - [k_1(w_{eq}^3 - w_i^3) + k_2(w_{eq}^2 - w_i^2) + k_3(w_{eq} - w_i)] \quad (4.18)$$

If the model is simulating the regeneration, the heat exchanged with the water flux is calculated using equation from the $\varepsilon - NTU$ method:

$$Q = \frac{Ec_w(T_{eq} - T_{w-in})}{v_l(1 - g_v)} \quad (4.19)$$

E is the effectiveness, at the denominator there is net volume occupied by the silica gel, not the void grade. From this, the outlet temperature of water is calculated as:

$$T_{w-out} = \frac{Q \cdot v_l(1 - g_v)}{c_w} + T_{w-in} \quad (4.20)$$

It is now possible to calculate the heat exchanged during the adsorption/regeneration:

$$H_{ads} = h_{ads}M_tA_s(x_{in} - x_{out}) - Q \quad (4.21)$$

For the adsorption the term Q will be 0. From this T_s and T_a are evaluated combining equations 4.10 and 4.11.

Auxiliary equations In many of the equations appearing in the model there are intermediate coefficients obtained from experimental regression found in literature.

Heat and mass transfer coefficients are calculated using [28]:

$$M_t = 1.7GRe^{-0.42}$$

$$H_t = 0.6GC_aRe^{-0.42}$$

where G is the specific flow rate expressed in kg/m^2s , Re is the Reynolds number and c_a is the specific heat. All the quantities are referred to the bulk air stream.

Adsorption heat of the water vapor is calculated in function of the water content of the bed [29]:

$$for w \leq 0.05 \quad \rightarrow \quad h_{ads} = 3500 - 13400w$$

$$for w > 0.05 \quad \rightarrow \quad h_{ads} = 2950 - 1400w$$

Air thermophysical properties are calculated using the following equations [30]:

$$\mu = (\mu_a x_a + \mu_v x_v) \left(1 + \frac{x_v - x_v^2}{2.75}\right)$$

where:

$$\begin{aligned} \mu_a &= 7.801\tau - 0.6266\tau^2 + 0.02942\tau + 0.00769\rho_a \\ \mu_v &= \frac{40.407}{\tau^2} - \frac{18.473}{\tau} + 3.853\tau + \rho_v \left(0.4077 - \frac{1.988}{\tau}\right) \\ x_a &= \frac{0.622072}{0.22072 + w} \\ x_v &= \frac{w}{0.622072 + w} \\ \tau &= \frac{T + 273.15}{100} \end{aligned}$$

Air specific heat is evaluated using [31]

$$c_a = 1.884m + 1.005(1 - m)$$

where:

$$m = \frac{w}{1 + w}$$

Silica gel specific heat is evaluated using [28]:

$$c_s = 4.178q + 0.921$$

Proceeding with the model calculation, the pressure drop in the heat exchanger is evaluated using the Ergun's equation. Pressure drop is generally a parameter that permits to quantify the energy consumption associated with the ventilation.

In a vertical fixed bed, with constant section, the velocity of the stream can be evaluated with the mean velocity being the section smaller enough not to develop the typical parabolic behaviour. Assuming that the particles have pseudospherical geometry with average diameter D , pressure drops are function of the bed depth L , vacuum degree ε and stream velocity.

The particles random distribution is called Random Close Packing, it generates a large number of vacuum pores between silica gel particles. This volume is identified as vacuum degree, defined as the ratio between the volume of vacuum and the total bed volume. According to Kepler's conjecture, the minimum ε obtainable is:

$$\varepsilon_{min} = 1 - \frac{\pi}{\sqrt{3}/2} \approx 25.95\%$$

In some studies ([32], [33]) it was demonstrated that for solid spheres pured randomly like in our case ε cannot exceed 36.6%.

In thix model an equation derived from Darcy relations on pressure drops for packed bed columns was used. It is valid in the case in which depth dimensions are greater than column diameter [34].

$$\Delta P = \left(\frac{150}{Re_{eff} + 1.75} \right) \left(\frac{L(1 - \varepsilon)}{\rho_a D \varepsilon^3} \right) \left(\frac{Q \rho_a^2}{3600 S} \right) \quad (4.22)$$

In a previous work, it was demonstrated that this model suits with the experimental results. Another consideration has to be done about the presence of fins that affect significantly the distribution on the spheres in the bed and consequently their void degree.

In literature, there is a study that takes in to consideration this aspect, developing a semiempirical relation for p/d ratio within the range of 1-1.95 [35].

$$\frac{p}{d} \leq 1.707 \rightarrow 1 - \varepsilon = \frac{\pi}{\frac{\gamma p}{d} \sqrt{4 \left[1 - \left(\frac{p}{d} - 1 \right)^2 \right] - 1}}$$

$$1.707 < \frac{p}{d} \leq 1.8164 \rightarrow 1 - \varepsilon = \frac{2\pi \left(2 - \frac{p}{d} \right)}{3\gamma \sqrt{3 - 4 \left(\frac{p}{d} - 1 \right)^2}}$$

$$1.8164 < \frac{p}{d} \leq 1.95 \rightarrow 1 - \varepsilon = \frac{2\pi}{3\gamma \sqrt{3 \frac{p}{d}}}$$

γ is an empirical coefficient of correction equal to 1.065, p is the distance between one fin and the other, d is the diameter of the spheres. In figure 4.5, a graphical evidence of the model equations.

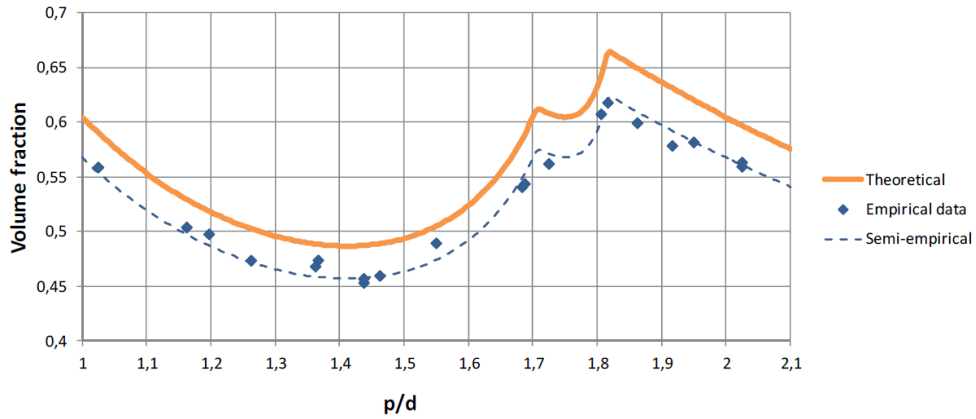


Figure 4.5: Volume fraction variation with respect to p/d ratio [35]

At this point, diffusion effects are calculated. This phenomenon in cannot be neglected for long period of adsorption and desorption since the vapour in this conditions has enough time to diffuse inside the particles. It has two opposite effects considering adsorption and regeneration:

- for adsorption diffusion has a positive effect since it enhance the water vapor to

get trapped inside the inner parts of silica gel spheres, decreasing its concentration on the external surface;

- for regeneration diffusion has a negative effect since it increases the energy necessary for desorption, acting as a resistance on mass transfer phenomenon.

To solve this problem and calculate the water vapor concentration in time through silica gel particles, an approximation of the convolution integral of Fundamental Solution was used.

$$W(x, t) = \int S(x - y, t, D) \cdot f(y) \cdot dy$$

S is the fundamental solution of transient diffusion problem without boundaries and source equal to zero, its evaluation is given in equation 4.23

$$S(x, t, D) = \frac{e^{-\frac{x^2}{4Dt}}}{\sqrt{4\pi D}} \quad (4.23)$$

D is the water vapor diffusivity in silica gel pores calculated in $[m^2/s]$, it is evaluated in function of T_s and water vapor concentration, the relation used to evaluate it is taken from literature [28].

$$D = D_0 \cdot e^{\frac{0.974 \cdot H_{ads} \cdot 10^{-3}}{T_s + 273.15}}$$

where D_0 is a constant value equal to $1.6 \cdot 10^{-6} m^2/s$

4.2.4 Model validation

In order to check the model reliability, a comparison with the experimental data was done both for adsorption and regeneration. This analysis was carried out putting in the model experimental data as input and check out the outputs obtained. Since the experimental data available belonged to the test-bench prototype, the model was adapted to it. Only the battery geometrical dimensions and the silica gel mass contained were adapted being the thermodynamic principle among the two prototypes exactly equal. The new dimensions used are $650 \times 650 \times 120 mm$ and the mass of silica gel, automatically calculated considering the new volume and the vacuum degree, is $28.45 kg$.

Adsorption Considering the adsorption process the experimental quantities used as inputs are:

- the inlet temperature of the air T_{in} ;
- the inlet absolute humidity of the air x_{in} ;
- the initial water content of the bed w_0 ;
- the air mass flow p_a , calculated considering equation 2.2 with fan regulation equal to 100% .

The quantity controlled as output were:

- the outlet temperature of the air T_{out}
- the outlet absolute humidity of the air x_{out}

The results, firstly obtained, showed good approximation for the temperatures but bad approximations for the absolute humidities.

The reasons for this discrepancy are thought to be mainly related to a bad modelling of the phenomenon of diffusion. In particular, the kinetics of diffusion seems to have a strong influence on the overall system. According to Aristov et al , [36], the linear diffusion models strongly underestimates the water uptake at short times and overestimates it for longer times. For the model purpose, that is mainly to quantify the water collected by the prototype, it can be considered acceptable to only consider the integral in time of the absolute humidity that according to the mass balance given in equation 4.9 can be calculated as follows:

$$w(t) = w_0 + \frac{\dot{m}_a}{m_s}(x_{in} - x_{out})t$$

Multiplying this quantity for the silica gel mass m_s we obtain the water content in kg inside the bed at time t . It was observed comparing the results obtained by the model with the experimental ones that in this case the model can be considered reliable, containing the error within the 10%.

Anyway it was found that inserting in the model a correction factor equal to 3.23 to the air flow, the results show a way better approximation also for the absolute humidities.

In this way the model seems to have a good approximation of the experimental data and so can be considered reliable for the purpose of the study.

Figures from 4.6 to 4.11 show the comparison of the validation of the absolute humidity and the temperature without (on the left) and with the correction factor (on the right).

It is possible to observe that the temperatures are not affected by the correction.

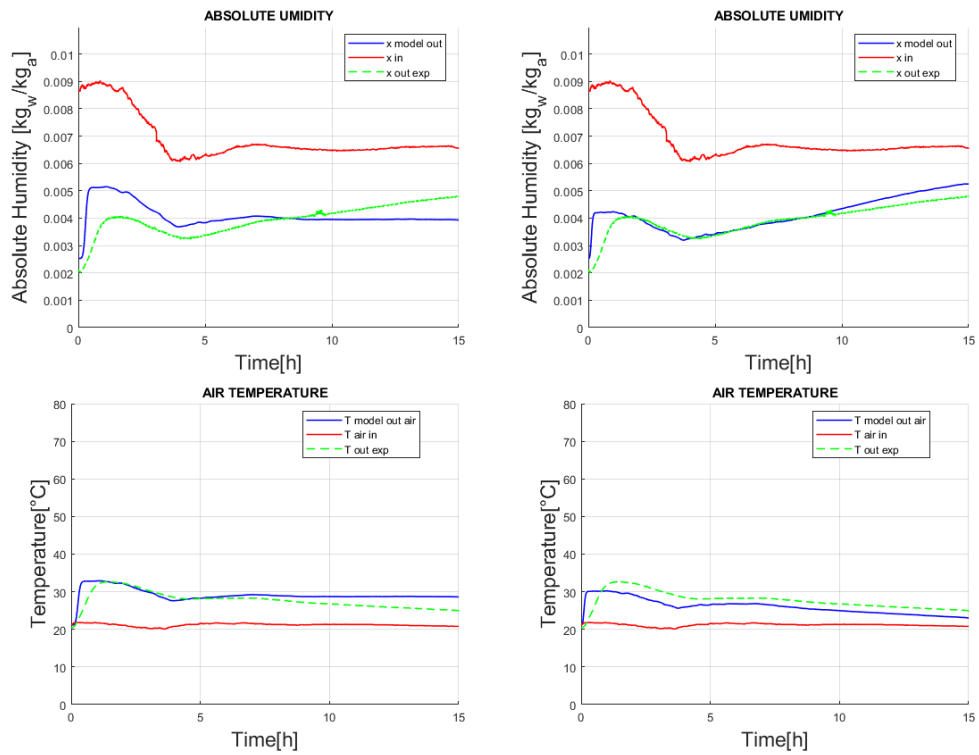


Figure 4.6: TEST 20-Validation

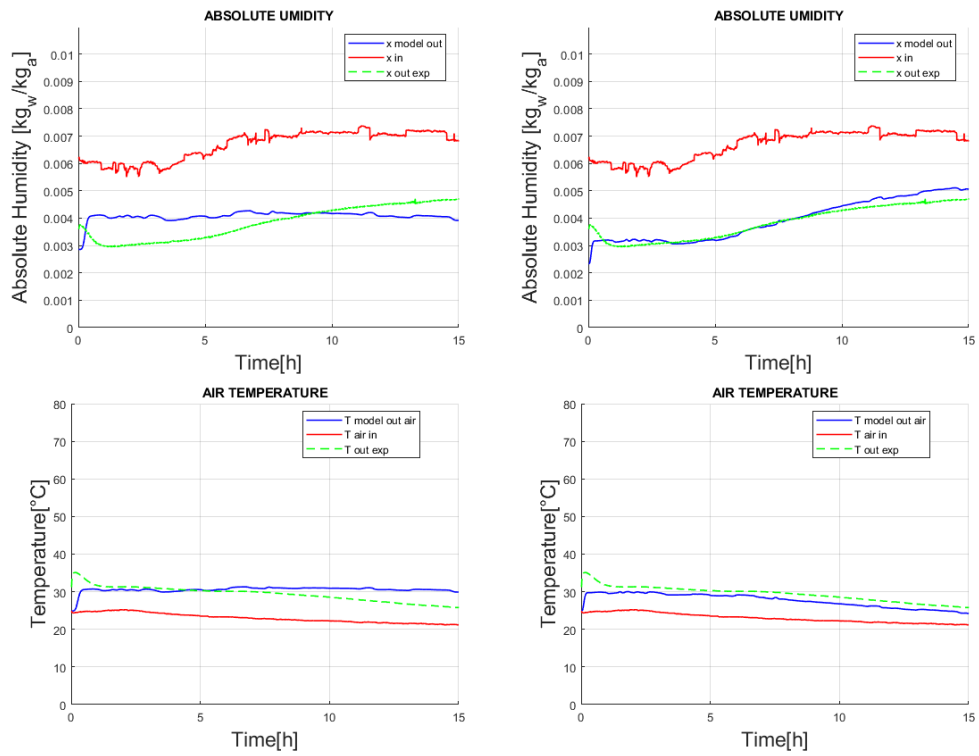


Figure 4.7: TEST 22-Validation

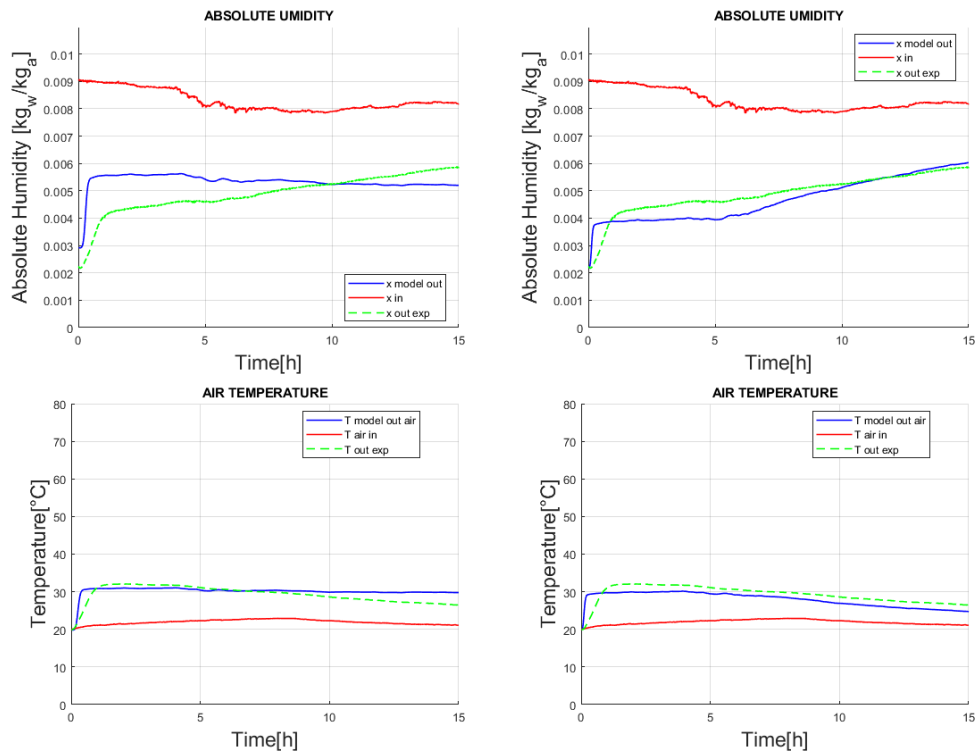


Figure 4.8: TEST 26-Validation

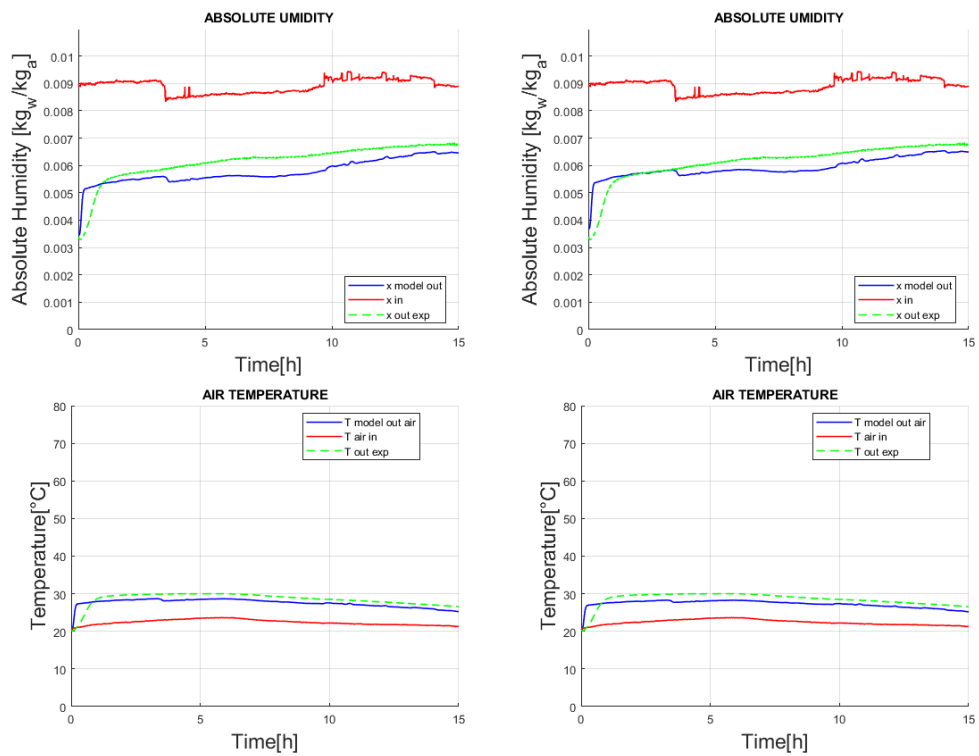


Figure 4.9: TEST 28-Validation

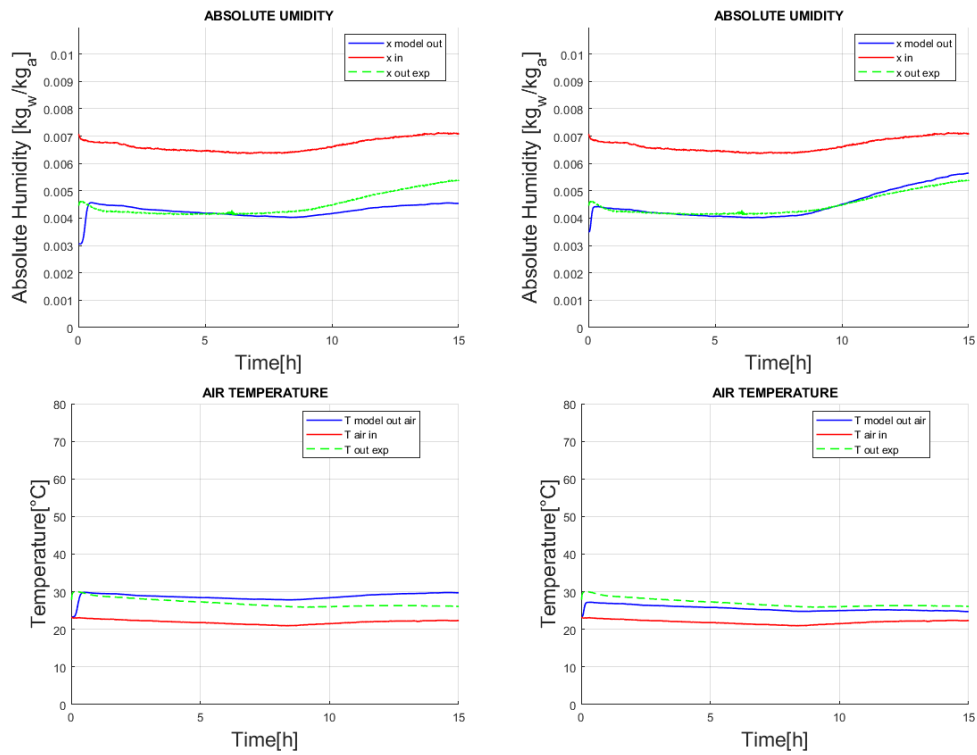


Figure 4.10: TEST 32-Validation

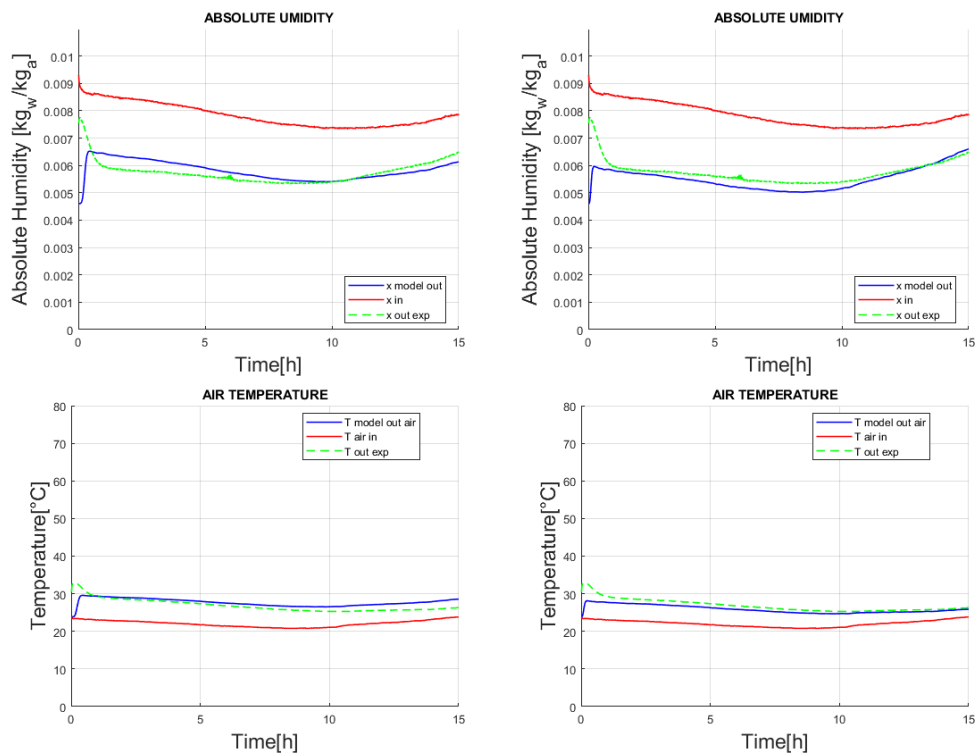


Figure 4.11: TEST 38-Validation

Regeneration Same consideration can be done for the regeneration phase. In this case, since the system works also coupled with the heat source also the water temperatures are concerned. The inputs are:

- the inlet temperature of the air T_{in} ;
- the inlet absolute humidity of the air x_{in} ;
- the inlet temperature of the water T_{w-in} ;
- the initial water content of the bed w_0 ;
- the air mass flow p_a , calculated considering equation 2.1 with fan regulation corresponding to the one used in the experimental test .

The output quantities of the model compared with the experimental value, in this case are:

- the outlet temperature of the air T_{out} ;
- the outlet absolute humidity of the air x_{out} ;
- the outlet temperature of the water T_{w-out} .

In this case the application of the correction factor to the air flow does not seem to improve the results of the model. For this reason it is not possible to consider this process validated. The reason for this can be related again to a bad modelling of the diffusion process. Also considering remembering the hypothesis done for the model, the mododimensionality for a system whose dimensions are not very thin is not a good approximation.

One test for each fan regulation is reported, from figure 4.12 to 4.15. It is possible to observe how increasing the fan regulation the results get worse.

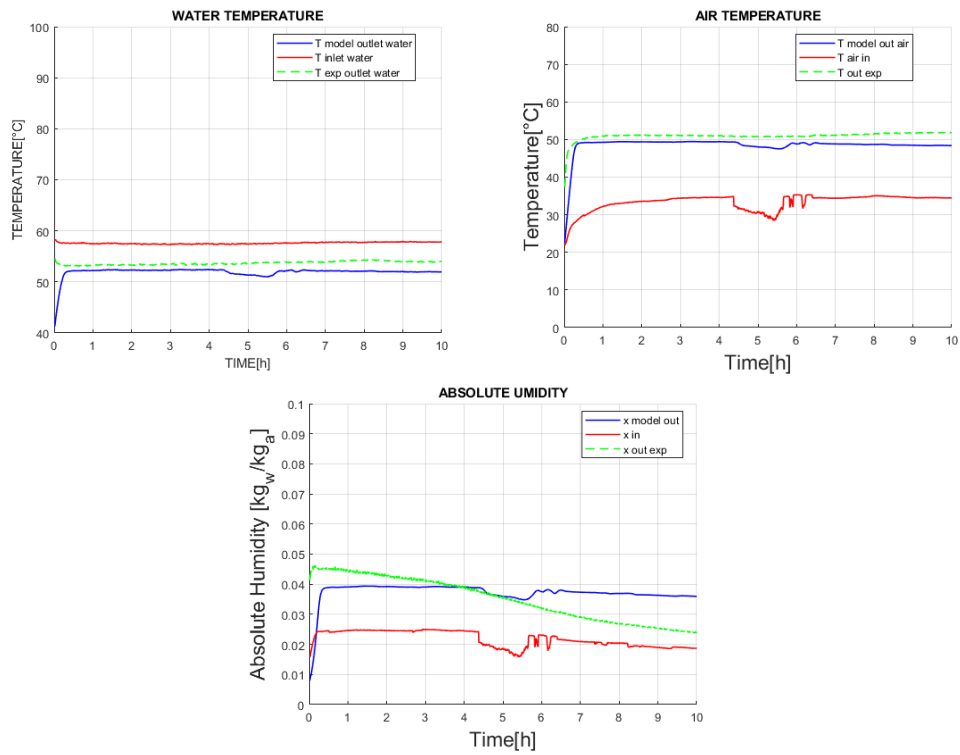


Figure 4.12: TEST 23 (fan regulation 30%)-Validation

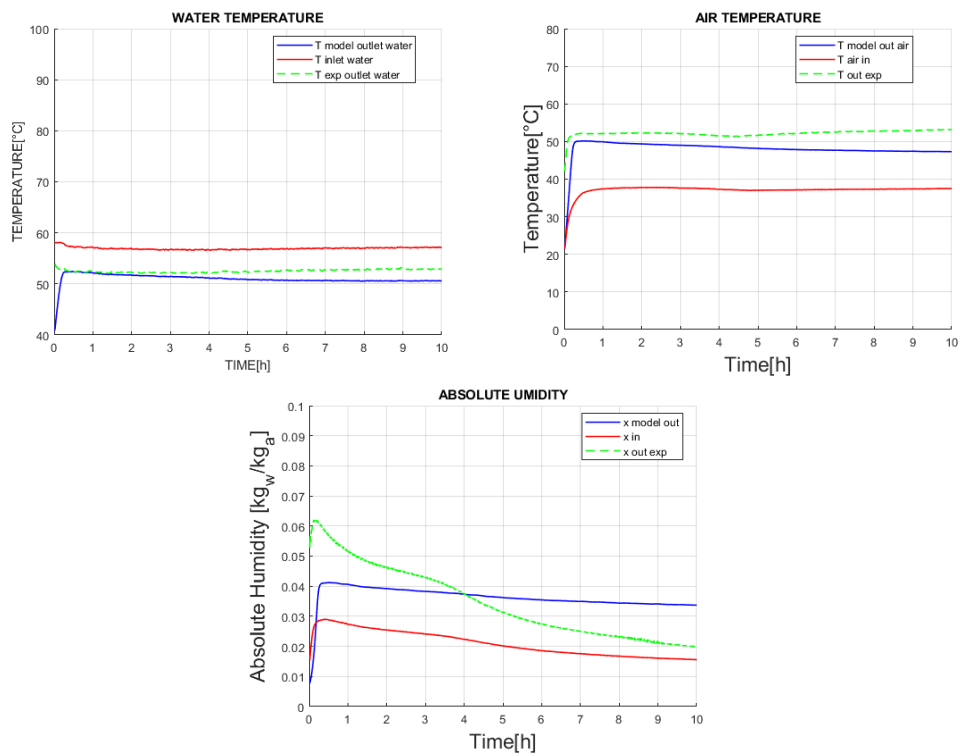


Figure 4.13: TEST 25 (fan regulation 50%)-Validation

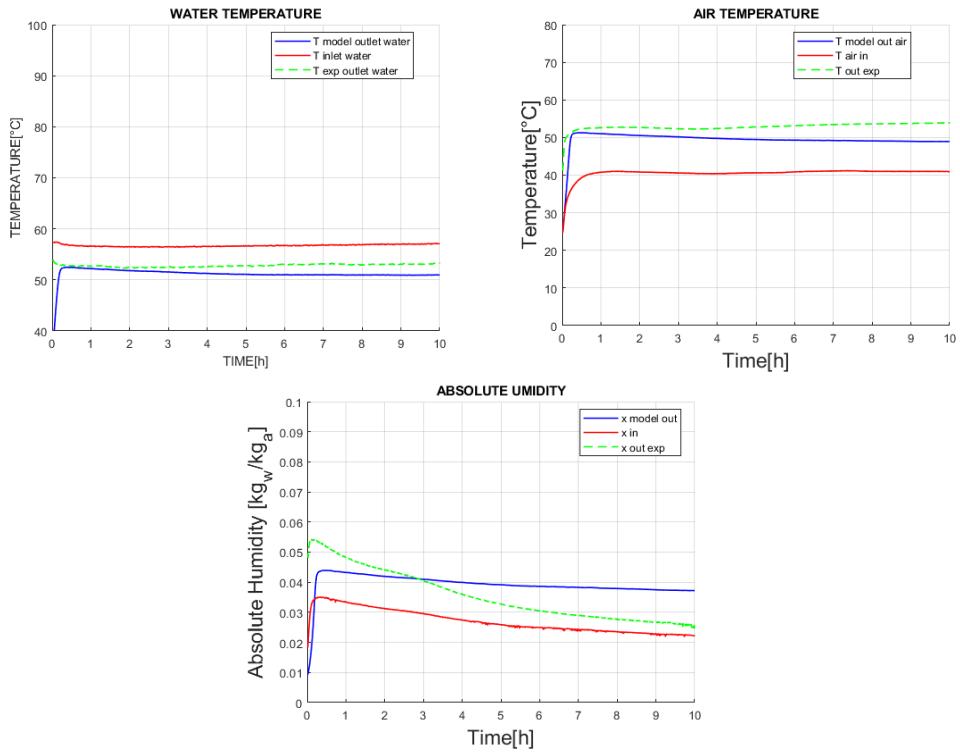


Figure 4.14: TEST 33 (fan regulation 70%)-Validation

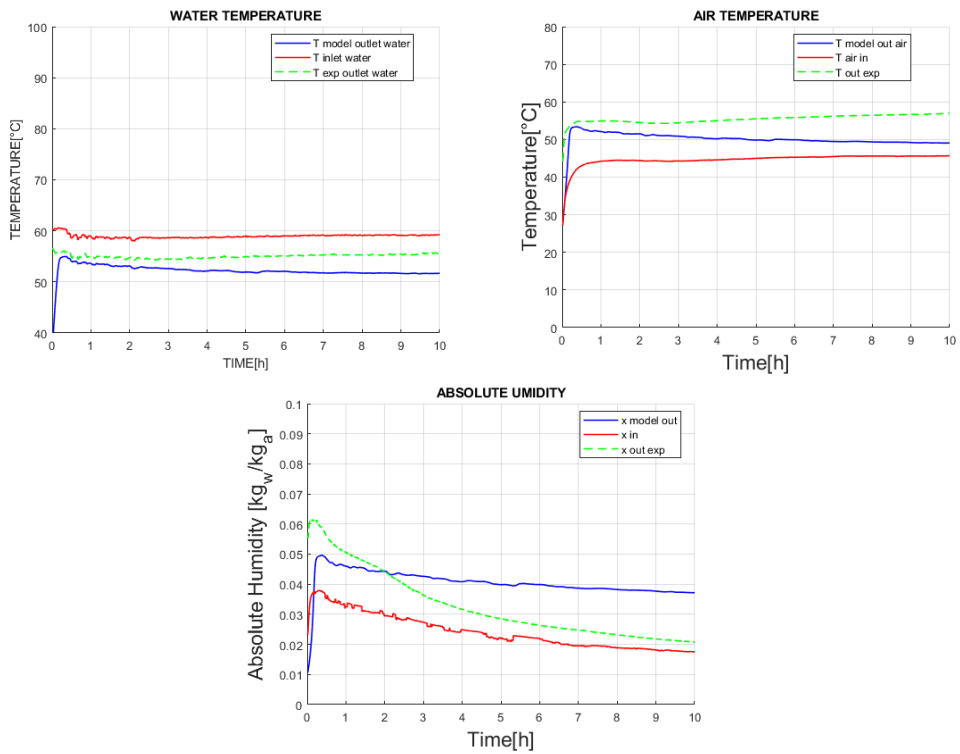


Figure 4.15: TEST 17 (fan regulation 90%)-Validation

Chapter 5

Results

The aim of the model explained in the previous chapter was to characterize the performances of the SAWG prototype in relation to different external condition. The charge and discharge phases were analyzed consequently, and it was studied how the mass changes in the range of ten days. During this period also the variables related to the collectors and the ones related to the air streams were checked. Inside the software TRNSYS, the climatic data files from all over the world are available from the *Meteonorm* database. After this analysis, some locations were chosen, trying to cover all the possible type of climatic zones that could match with an area that suffers from physical or economical water scarcity, as seen in figure 1.10. For each location four days of the year are taken into account representative of the four seasons : the 15th of January, the 15th of April, the 15th of July and the 15th of October. It was ensured that the selected day was sunny for most of the daytime so that within 24h both adsorption and regeneration could be performed.

5.1 Tunisi sample

Before comparing each location, 10 days of July in Tunisi were analyzed as sample in order to check the charge/discharge phases along few days. Also the performances of the panels and the variables related to the air stream were plotted. Since the plots are taken directly from TRNYS they are not detailed with units of measurements. Each figure will be better explained in detail.

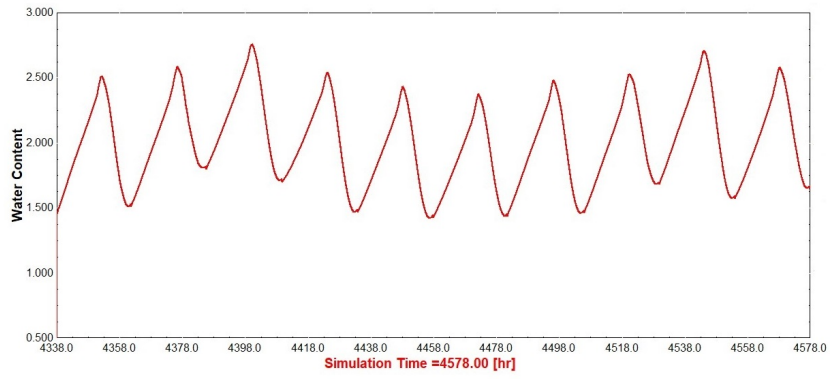


Figure 5.1: Water content variation

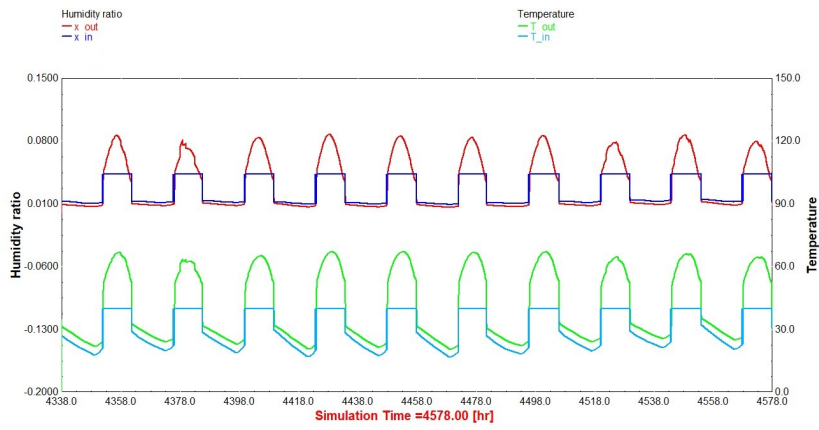


Figure 5.2: HX-ADS air inlet and outlet

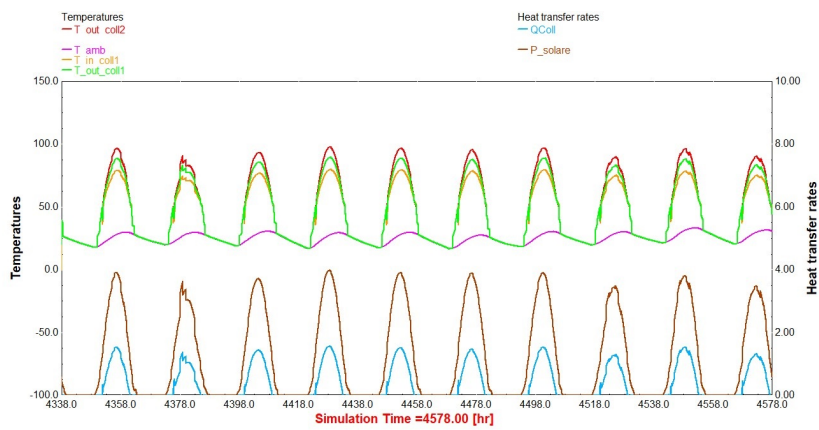


Figure 5.3: Collector variables

In figure 5.1, the mass variation of the water inside the bed in lt is plotted, from the 1st of July to the 15th of July. This quantity is obtained multiplying the relative water content of the bed times the mass of dry silica with which the HX-ADS of the SAWG prototype is filled. It is possible to observe how the water content of the bed maintains a regular trend, going from a maximum of 2.7 lt to a minimum of 1.5 lt and so producing each day approximately 1.2 lt of water considering the system working with one battery. During this month the days show a similar behaviour the one with the other, and so they permit to always have sufficient thermal energy to perform the complete regeneration. It would not be possible in case of cloudy days instead.

In figure 5.2, the variables relative to the HX-ADS air streams are plotted. On the left axis, x_{in} (in blue) and x_{out} (in red) are plotted in $[kg_w/kg_s]$. It is possible to clearly distinguish the adsorption phase, in which the absolute humidity variation is much lower, from the regeneration in which the variation is much bigger. This is due to the fact that regeneration is enhanced by the solar thermal energy. As a matter of fact, it becomes also evident how the humidity ratio exiting the heat exchanger follows the solar radiation behaviour during the daily hours. Same consideration can be done for the temperatures. On the right axis, T_{air-in} and $T_{air-out}$ are plotted in $[^{\circ}C]$, respectively in light blue and green. During the adsorption phases they maintain an almost constant difference, while during regeneration $T_{air-out}$ shows a behaviour similar to the daylight.

Finally, in figure 5.3, the quantities related to solar collectors are plotted. On the left axis, we find the temperatures in $^{\circ}C$ of the water entering the first collector ($T_{in\ coll}$) in yellow, the temperature of the water exiting the first collector ($T_{out\ coll\ 1}$) in green and the temperature of the water exiting the second panel ($T_{out\ coll\ 2}$) in red. In pink the ambient temperature is plotted. It is possible to notice an overall $\Delta T = 20^{\circ}C$, equally distributed among the two collectors. On the right axis, we find heat rates expressed in kW. In brown the total surface irradiance is plotted and multiplied by the area of the collectors, in light blue the heat rate absorbed by the system is calculated.

5.2 Climate zones comparison

Once the average behaviour of the sistem was checked, an analysis comparing different possible performances was carried on. First of all, seven different locations from all over the world belonging to different climate zones, according to figure 5.4 were chosen. In table 5.1, the cities chosen and relative climate zone are shown.

City	Country	Climatic Zone
Bamako	Mali	Arid/Semi-arid
Bangkok	Thailand	Tropical Wet and Dry
Bluefields	Nicaragua	Tropical
Lisbon	Portugal	Mediterranean
Perth	Australia	Arid/Semi-arid
Torino	Italy	Mediterranean
Tunisi	Tunisia	Arid/Semi-arid

Table 5.1: Representative cities for each climate zone

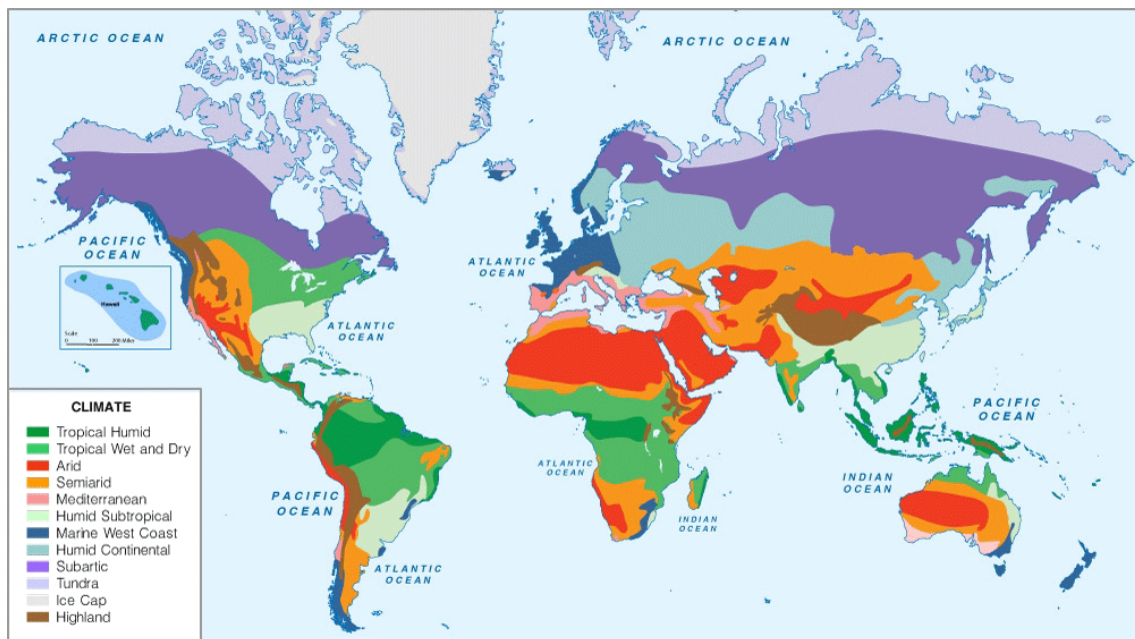


Figure 5.4: World climate zones

For each city, a daily simulation was performed. In order to have a complete adsorption phase the starting time of the calculation is around 6.00 pm when the sun sets, and a low initial relative water content was set. In this way during the night the adsorption goes on, it stops when the temperature of the water flowing inside the collectors start to raise.

Having daily information available, the following quantities were analyzed:

- **WP** the daily water production [lt];
- **CS** the specific consumption that is the energy needed to collect 1 lt of water [kWh/lt]. Only thermal power was considered, since as it was seen in data analysis of the test bench prototype, electric power is negligible with respect to the thermal one.

Furthermore the average relative humidity (RH), is plotted too since it helps to understand the quantity of moisture available in the air during the chosen day. Also the percentage time of the day in which regeneration or adsorption are performed, have been plotted. This quantity helps to quantify the time needed from each phase.

Grouping the cities in macro-climate zones, the following results are obtained.

Tropical Climate Tropical climates are typically characterized by a non-arid climate in which temperatures are generally constant and above 18.4°C. These areas are characterized by only two seasons throughout the year: wet season and dry season. Sunlight is predominantly intense. Both in Bangkok and Bluefields, the climate is very humid during the whole year so there are not big variations on the performances of the prototype during the year. These areas seem to be the most favorable zones for the application of the prototype. The production of water is never below 1.6 lt/day and the specific consumption associated to it is never above 6.3 kWh/lt.

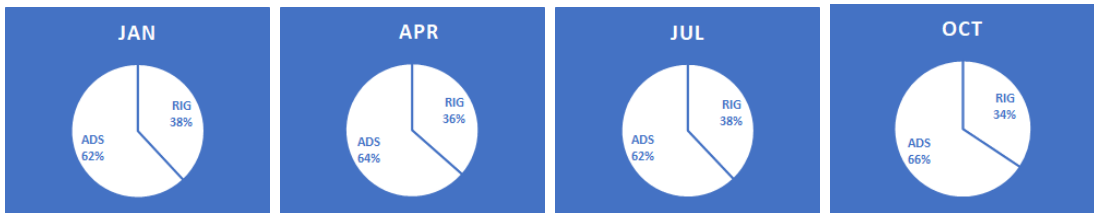
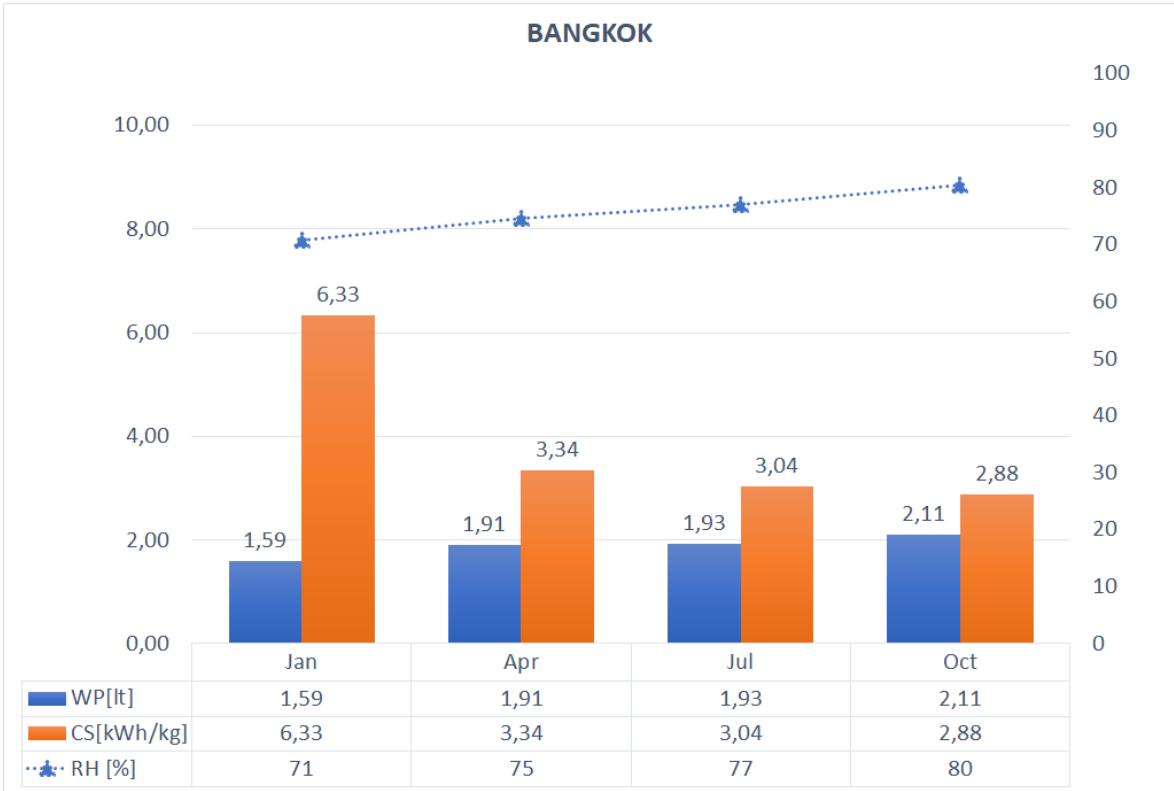


Figure 5.5: Bangkok

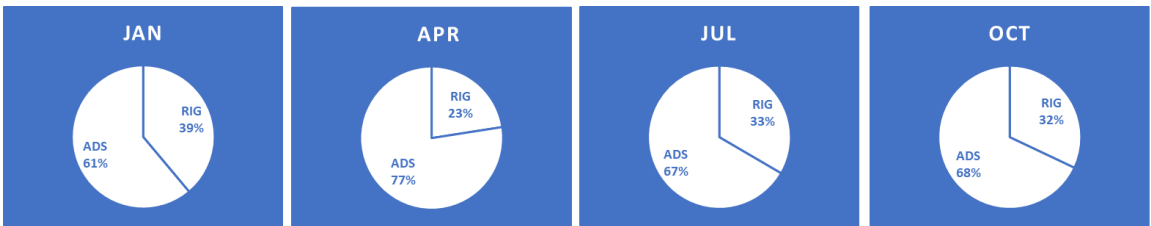


Figure 5.6: Bluefields

Arid or semiarid climate This type of climate is classified according to the level of precipitation being below potential evapotranspiration. So it is characterized by very dry climate and big variation in terms of air temperature. The sunlight is constantly high. We can distinguish among two type of seasons: in January and April the relative humidity is very low and so it the water production (up to 0.48 lt/day). This tipe of climate is generally quite unfavorable for the application of an atmospheric water generator. As a consequence of the low amount of water produced, very high specific consumptions are shown. On the other hand in July and October the situation is opposite.

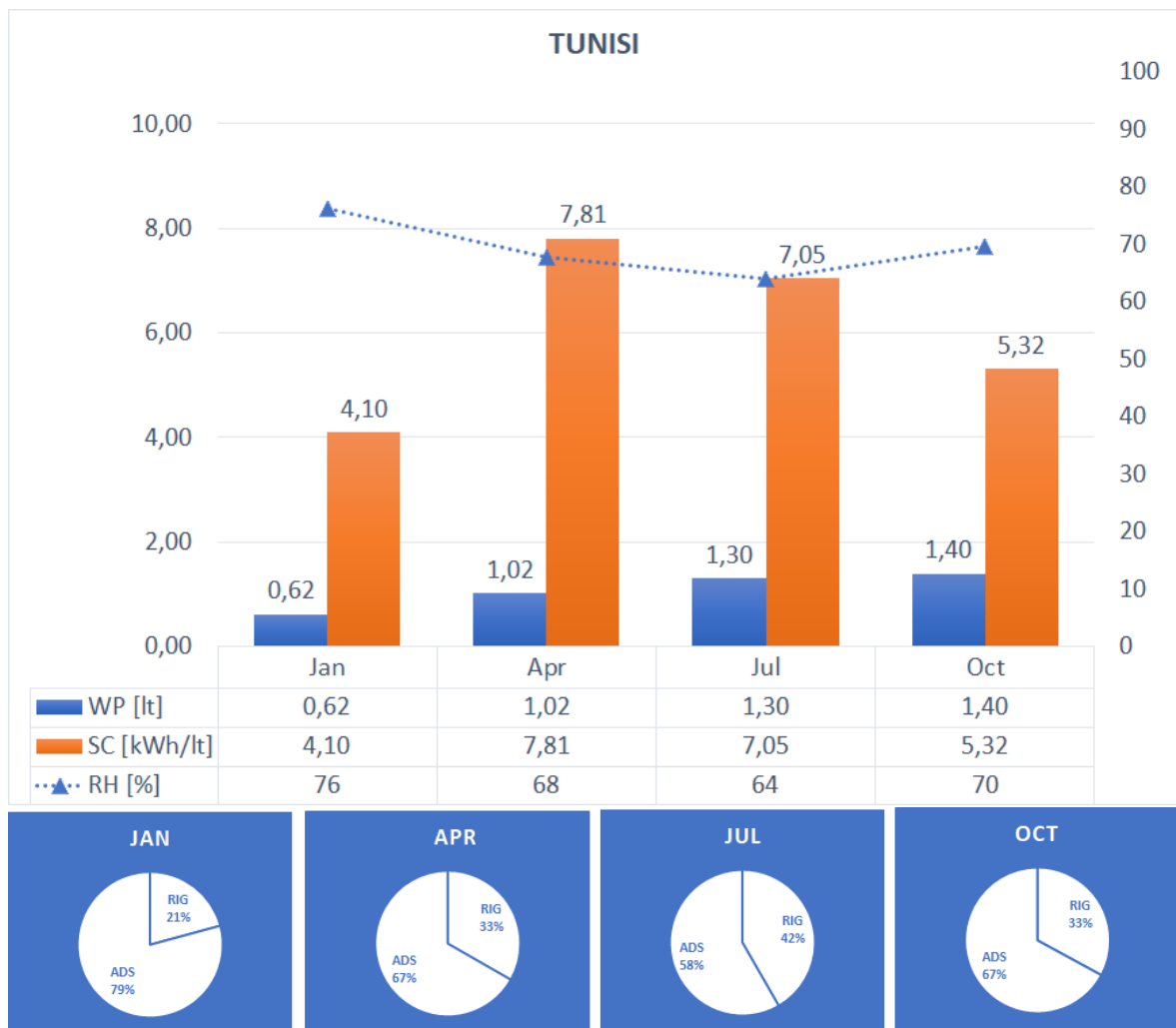


Figure 5.7: Tunisi

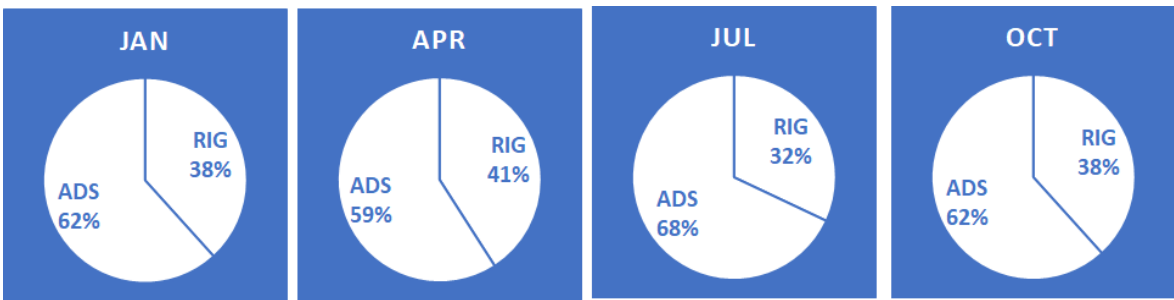
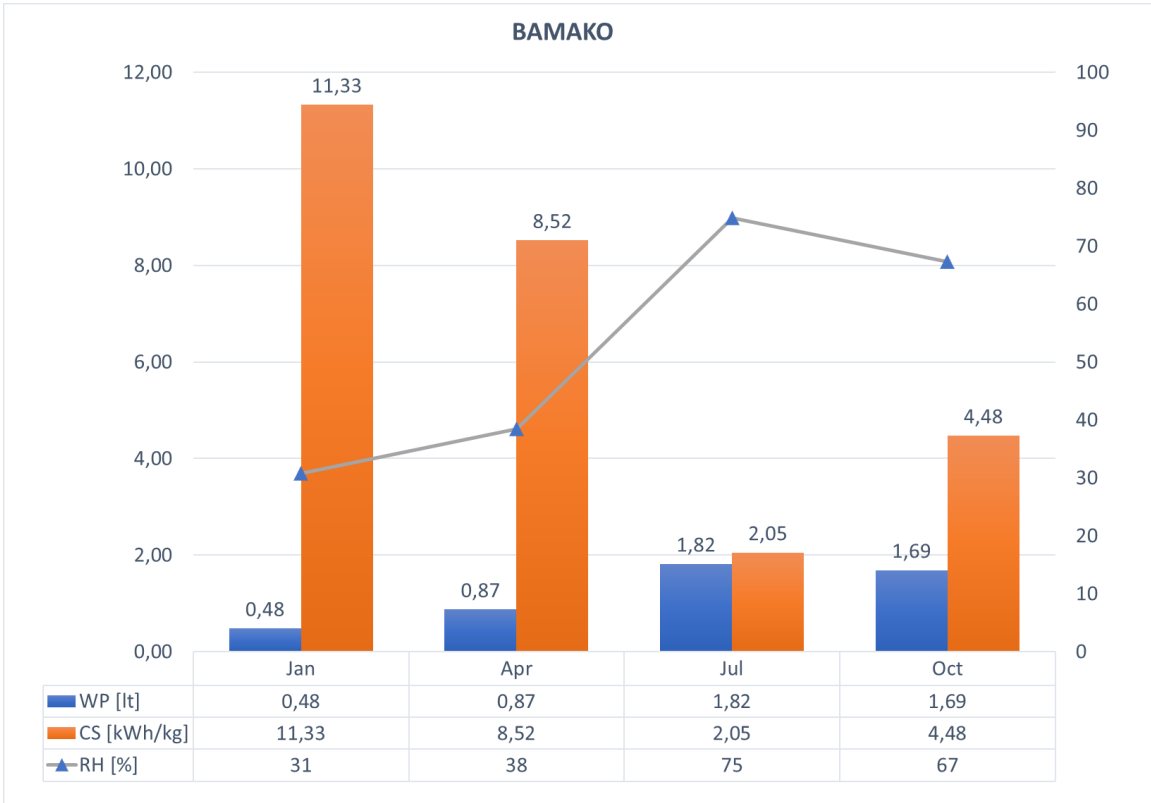


Figure 5.8: Bamako

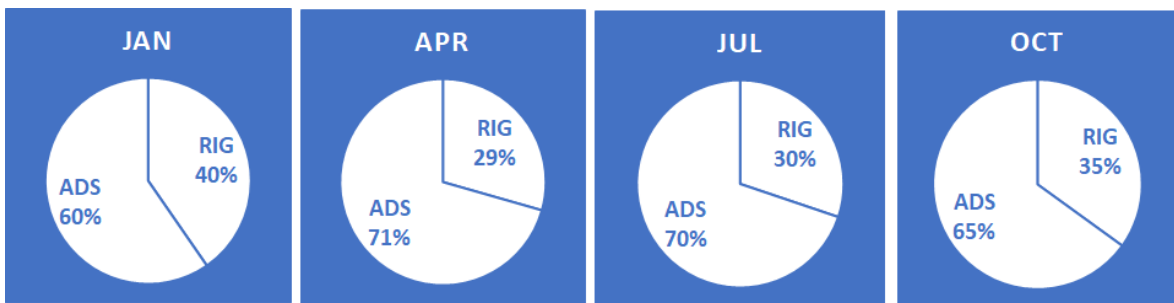
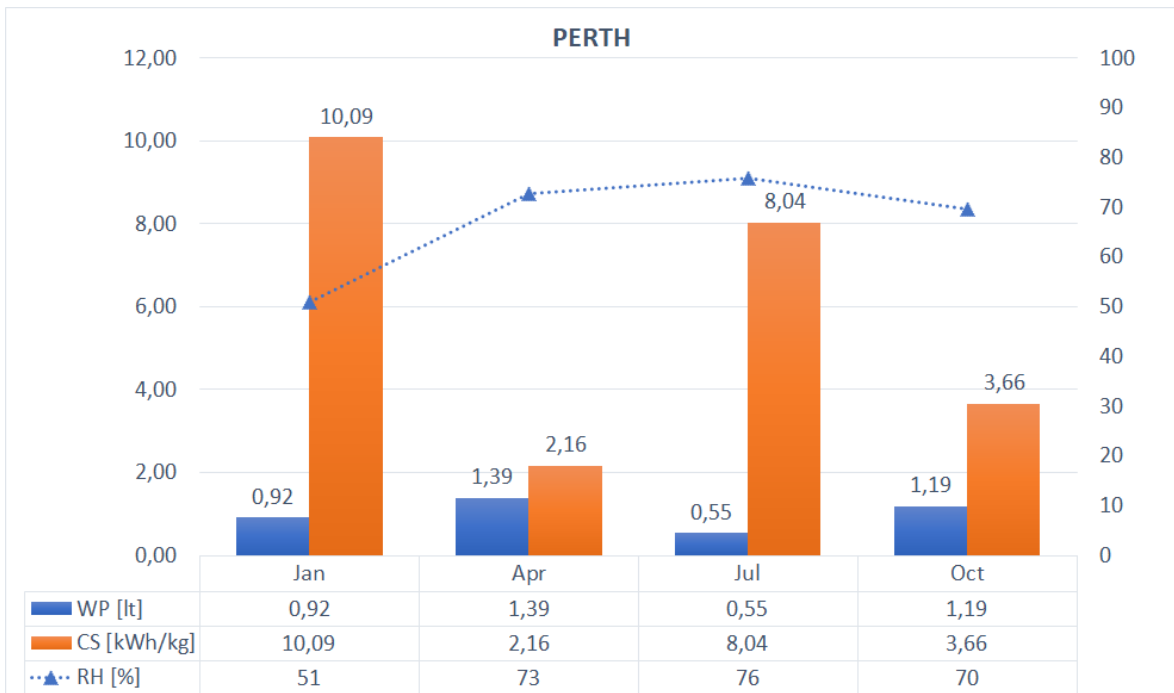


Figure 5.9: Perth

Mediterranean climate As for Mediterranean climate, Lisbon and Turin were taken into account. This type of climate is characterized by rainy winters and dry summers, in fact the performances of the prototype change considerably during the year. For both locations chosen, the water uptake goes from a minimum of 0.41 lt/day to a maximum of 1.5/day lt. This areas shows an intermediate behaviour with respect to the tropical and the arid ones.



Figure 5.10: Lisbona

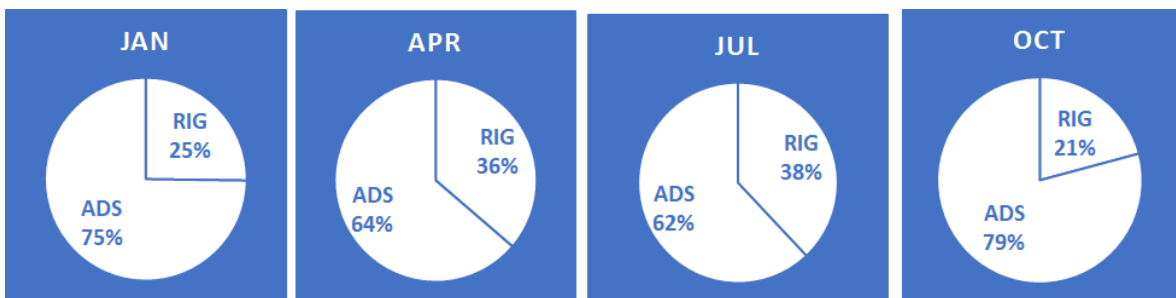


Figure 5.11: Torino

Chapter 6

Conclusions

The aim of the work was to optimize the performances of the water generator prototype SAWG. This was possible through a previous data analysis of the test bench prototype. The results of this first analysis showed typical trends of variables during adsorption and regeneration. The variables on which the focus was concentrated were mainly the ones that characterize the performances of the HX-ADS. These variables are the inlet and outlet temperature, relative humidity and absolute humidity of the air stream. Other variables investigated were the dew point temperature, whose comparison with ambient temperature permits to make consideration on the feasibility of condensation; the mass balance, and the specific consumption of the prototype. This last quantity permits a comparison with the other prototypes already existing, whose data were taken from literature.

An analysis on how different fan regulations during regeneration affect the specific consumption was carried on. It was shown that it was not useful to quantify the energetic performances of the prototype. The electricity consumption related to the fans is very marginal with respect to the thermal consumption that is the same for the different fan regulations.

With the data collected it was possible to build the model and adapt it to the prototype features.

The results of the model show, as expected, a variation in terms of performances of the prototype for different climatic zones. It was seen how the water uptake change from a maximum of 2.2 lt/day in tropical areas, to a minimum of 0.48 lt/day in arid

climates. Of course, water production is strictly related to the moisture content of the external air.

As well as for the specific consumption, it reaches a peak of 11 kWh/lt in Bamako (Mali) that corresponds to the lower water production among the simulations performed. The minimum value for specific consumption is reached in the simulation carried in Bluefields (Nicaragua) with a value of 0.7 kWh/lt.

These results were obtained considering only one of the two HX-ADS installed on the prototype. For sure, increasing the available sorbent material, the water uptake should increase considerably as well.

As future work, it could be interesting to investigate an optimization of the performances with two batteries implementing a suitable controller logic that aims to maximize the water production and minimize the consumption.

Bibliography

- [1] <https://www.un.org/sustainable-development/water-and-sanitation/>.
- [2] United Nations. *Water for a sustainable world*. 2015.
- [3] M M Faridb, J R Selmana, and Said Al-hallaj. Solar desalination with a humidification-dehumidification technique - a comprehensive technical review. 160:167–186, 2004.
- [4] UN. Back to our Common Future: Sustainable Development in the 21st Century (SD21) project. *Back to our Common Future: Sustainable Development in the 21st Century (SD21) project*, page 39, 2012.
- [5] Iv Com. INVESTING IN WATER AND SANITATION: INCREASING ACCESS, REDUCING INEQUALITIES Special Report for the Sanitation and Water for All (SWA) High-Level Meeting (HLM) 2014 WHO Library Cataloguing-in-Publication Data. 2014.
- [6] <https://www.groundwater.org/>.
- [7] Igor S. Zektser and Lorne G. Everett. *134433E*. United Nations Educational, Scientific and Cultural Organization, 2004.
- [8] Mahmoud Shatat, Mark Worall, and Saffa Riffat. Opportunities for solar water desalination worldwide: Review. *Sustainable Cities and Society*, 9:67–80, 2013.
- [9] A M K El-ghonemy. Fresh water production from / by atmospheric air for arid regions , using solar energy : Review. 16:6384–6422, 2012.

- [10] M. Eslami, F. Tajeddini, and N. Etaati. Thermal analysis and optimization of a system for water harvesting from humid air using thermoelectric coolers. *Energy Conversion and Management*, 174(April):417–429, 2018.
- [11] Onur Ozkan, Enakshi D Wikramanayake, and Vaibhav Bahadur. Modeling humid air condensation in waste natural gas-powered atmospheric water harvesting systems. *Applied Thermal Engineering*, 118:224–232, 2017.
- [12] Bathina Chaitanya, Vaibhav Bahadur, Ajay D. Thakur, and Rishi Raj. Biomass-gasification-based atmospheric water harvesting in India. *Energy*, 165:610–621, 2018.
- [13] Vincenzo Gentile, Marco Simonetti, Pietro Finocchiaro, and Gian Vincenzo Fraccastoro. Water production from the atmosphere in arid climates using low grade solar heat.
- [14] M Muselli, D Beysens, and I Milimouk. A comparative study of two large radiative dew water condensers. 64:54–76, 2006.
- [15] Farshid Bagheri. Performance investigation of atmospheric water harvesting systems. *Water Resources and Industry*, 20(August):23–28, 2018.
- [16] D. Bergmair, S. J. Metz, H. C. De Lange, and A. A. van Steenhoven. System analysis of membrane facilitated water generation from air humidity. *Desalination*, 2014.
- [17] D Bergmair, S J Metz, H. C. De Lange, and A. A. Van Steenhoven. A low pressure recirculated sweep stream for energy efficient membrane facilitated humidity harvesting. *Separation and Purification Technology*, 150:112–118, 2015.
- [18] A Magrini, L Cattani, M Cartesegna, and L Magnani. Production of water from the air: The environmental sustainability of air-conditioning systems through a more intelligent use of resources. The advantages of an integrated system. In *Energy Procedia*, volume 78, pages 1153–1158. Elsevier B.V., 2015.

- [19] Anna Magrini, Lucia Cattani, Marco Cartesegna, and Lorenza Magnani. Water production from air conditioning systems: Some evaluations about a sustainable use of resources. *Sustainability (Switzerland)*, 9(8), 2017.
- [20] Ben Gido, Eran Friedler, and David M Broday. Assessment of atmospheric moisture harvesting by direct cooling. *Atmospheric Research*, 182:156–162, 2016.
- [21] Nasrin Fathollahzadeh Attar, Keivan Khalili, Javad Behmanesh, and Neda Khanmohammadi. On the reliability of soft computing methods in the estimation of dew point temperature : The case of arid regions of Iran. *Computers and Electronics in Agriculture*, 153(August):334–346, 2018.
- [22] J. Y. Wang, R. Z. Wang, Y D Tu, and L W Wang. Universal scalable sorption-based atmosphere water harvesting. *Energy*, 165:387–395, 2018.
- [23] J. G. Ji, R. Z. Wang, and L. X. Li. New composite adsorbent for solar-driven fresh water production from the atmosphere. *Desalination*, 212(1-3):176–182, 2007.
- [24] Hyunho Kim, Sungwoo Yang, Sameer R Rao, Shankar Narayanan, Eugene A Kapustin, Hiroyasu Furukawa, Ari S Umans, Omar M Yaghi, and Evelyn N Wang. Water harvesting from air with metal-organic frameworks powered by natural sunlight. 434(April):430–434, 2017.
- [25] J. Y. Wang, J Y Liu, R. Z. Wang, and L W Wang. Experimental research of composite solid sorbents for fresh water production driven by solar energy. *Applied Thermal Engineering*, 121:941–950, 2017.
- [26] N Yu, R Z Wang, Z S Lu, and L W Wang. Development and characterization of silica gel – LiCl composite sorbents for thermal energy storage. 111:73–84, 2014.
- [27] Duc Thuan, Aqdas Nida, Kim Choon, and Kian Jon. Water vapor permeation and dehumidification performance of poly (vinyl alcohol)/ lithium chloride composite membranes. *Journal of Membrane Science*, 498:254–262, 2016.
- [28] A A Pesaran, A F Mills Seri, and Solar Energy. Moisture Transport in Silica Gel Packed Beds. 1986.

- [29] X J Zhang, Y J Dai, and R Z Wang. A simulation study of heat and mass transfer in a honeycombed rotary desiccant dehumidifier. *23:989–1003*, 2003.
- [30] J. Niu and L Zhang. Performance comparisons of desiccant wheels for air dehumidification and enthalpy recovery. *Applied Thermal Engineering*, *23:1347–1367*, 2002.
- [31] P. Ballany. Refrigeration and Air conditioning. 6th editio, 1983.
- [32] Macro-encapsulated P C M F O R Dehumidification. HEAT AND MASS TRANSFER IN A COMPOSITE BED OF SILICA GEL AND MACRO-ENCAPSULATED PCM FOR 1 Introduction. (March 2016).
- [33] P. Krishna, D. Pandey, and U.C. Cardiff. Close packed structure. *International Union of Crystallography*, 2001.
- [34] E. Sabri. Fluid flow through packed columns. *Chemical Engineer Progress*, *48*, 1952.
- [35] L. Pistocchini, S. Garrone, and M. Motta. Fluid dynamics optimization of a novel isothermal adsorption dehumidification system for solar driven applications. *Energy Procedia*, 2014.
- [36] Yuri I Aristov, Mikhail M Tokarev, Angelo Freni, Ivan S Glaznev, and Giovanni Restuccia. Kinetics of water adsorption on silica Fuji Davison RD. *1387:65–71*, 2006.